energies

MDPI

Review

Simulation and Optimization of Lignocellulosic Biomass Wet- and Dry-Torrefaction Process for Energy, Fuels and Materials Production: A Review

Antonios Nazos [1], Dorothea Politi [2], Georgios Giakoumakis [2] and Dimitrios Sidiras [2,*]

[1] Department of Mechanical Engineering, University of West Attica, 250 Thivon & P. Ralli, 12241 Egaleo, Greece
[2] Laboratory of Simulation of Industrial Processes, Department of Industrial Management and Technology, School of Maritime and Industrial Studies, University of Piraeus, 80 Karaoli & Dimitriou, 18534 Piraeus, Greece
* Correspondence: sidiras@unipi.gr; Tel.: +30-21-04-142-360

Abstract: This review deals with the simulation and optimization of the dry- and wet-torrefaction processes of lignocellulosic biomass. The torrefaction pretreatment regards the production of enhanced biofuels and other materials. Dry torrefaction is a mild pyrolytic treatment method under an oxidative or non-oxidative atmosphere and can improve lignocellulosic biomass solid residue heating properties by reducing its oxygen content. Wet torrefaction usually uses pure water in an autoclave and is also known as hydrothermal carbonization, hydrothermal torrefaction, hot water extraction, autohydrolysis, hydrothermolysis, hot compressed water treatment, water hydrolysis, aqueous fractionation, aqueous liquefaction or solvolysis/aquasolv, or pressure cooking. In the case of treatment with acid aquatic solutions, wet torrefaction is called acid-catalyzed wet torrefaction. Wet torrefaction produces fermentable monosaccharides and oligosaccharides as well as solid residue with enhanced higher heating value. The simulation and optimization of dry- and wet-torrefaction processes are usually achieved using kinetic/thermodynamic/thermochemical models, severity factors, response surface methodology models, artificial neural networks, multilayer perceptron neural networks, multivariate adaptive regression splines, mixed integer linear programming, Taguchi experimental design, particle swarm optimization, a model-free isoconversional approach, dynamic simulation modeling, and commercial simulation software. Simulation of the torrefaction process facilitates the optimization of the pretreatment conditions.

Keywords: biomass; lignocellulose; optimization; simulation; torrefaction

Citation: Nazos, A.; Politi, D.; Giakoumakis, G.; Sidiras, D. Simulation and Optimization of Lignocellulosic Biomass Wet- and Dry-Torrefaction Process for Energy, Fuels and Materials Production: A Review. *Energies* **2022**, *15*, 9083. https://doi.org/10.3390/en15239083

Academic Editors: Eliseu Monteiro and Sérgio Ferreira

Received: 26 October 2022
Accepted: 26 November 2022
Published: 30 November 2022

1. Introduction

Among the various renewable energy sources, lignocellulosic biomass (agricultural waste and forest residues), can successfully substitute fossil fuels and reduce greenhouse gas emissions, while torrefaction, a thermochemical pretreatment, can be used to upgrade raw biomass properties, reducing its transportation costs. Torrefaction research should focus on kinetics, particle sizing, and reactor modeling/design [1]. Torrefaction enhances biomass properties, such as energy density, mass and energy yield, moisture content, and particle size, facilitating its use for further processing, e.g., combustion, gasification, and co-firing with conventional fuel [2]. The biochar (torrefied solids) quality is defined by the heat processing parameters, in the lack or not of oxygen. Torrefaction technology can be useful for biofuel production industrial plants, such as farms, combined heat and power plants, and pulp/paper units. Torrefaction product properties, reaction mechanisms, technologies, and reactors should be considered to decide which torrefaction technology is preferable in each case [3].

The torrefaction-related research focuses on the effect on lignocellulosic biomass properties, energy densification, and solid/energy yields. Moreover, it deals with the industrial,

environmental, and agricultural effects of the lignocellulosic biomass torrefaction in combination with combustion, pyrolysis [4–7], liquefaction [8], gasification [9–12], and pollutants adsorption [13–16]. Furtherly, the research focuses on the torrefaction mechanism [17–19] understanding and its effect on the lignocellulosic structure [20–26]. In addition, several researchers have tried to understand the thermal degradation of lignocellulosic through kinetic models' application [27–38].

According to the above numerous review papers related to biomass torrefaction technology, torrefaction treatment is aimed at the production of energy, fuels, and materials. Especially, oxidative and non-oxidative dry torrefaction focuses on improving lignocellulosic biomass solid residue heating properties, while wet torrefaction, (so-called autohydrolysis, hydrothermal carbonization, hydrothermal torrefaction, hot water extraction, hydrothermolysis, hot compressed water treatment, water hydrolysis, aqueous fractionation, aqueous liquefaction, solvolysis/aquasolv, pressure cooking, acid-catalyzed wet torrefaction, or acid hydrolysis) attempts to maximize the fermentable to bioethanol monosaccharides and oligosaccharides production as well to improve the solid residue heating value. This review deals with the simulation and optimization of dry- and wet-torrefaction pretreatment of lignocellulosic residues such as straws, husks, stalks, peels, sawdust, shavings, chips, and pruning. The novelty of this present work is the systematic examination of the various torrefaction process simulation approaches existing in the international literature. Moreover, this paper emphasizes the use of simulation models for the optimization of the torrefaction process conditions with simultaneous maximization of the product yields in combination with enhanced products' properties.

2. Torrefaction Processes Classification

2.1. Dry Torrefaction

The major goal of the lignocellulosic biomass torrefaction processes is to upgrade the feedstock and produce mainly solid fuels with enhanced properties. The torrefaction processes can be classified as (i) dry [7,39–41], (ii) wet [39–42], (iii) steam [43–45], and (iv) microwave-assisted torrefaction [46–49]. Dry torrefaction can be classified as (a) oxidative [50,51] or (b) non-oxidative [51–53]. On the other hand, wet torrefaction can be applied using water, (a) without any catalyst, or (b) catalyzed by (i) acids (e.g., H_2SO_4 [54–58], H_3PO_4, succinic acid [55], HCl [59], acetic acid [60]), (ii) ammonia [61,62] or (iii) salts (e.g., NaCl, LiCl [60]). As regards dry torrefaction, lignocellulosic biomass can be processed in an inert non-oxidative atmosphere (using, e.g., nitrogen), or in a common oxidative atmosphere (in the presence of oxygen), at 200–300 °C [17,63–68]. As regards wet torrefaction, lignocellulosic biomass can be processed using water (with or without a catalyst) at 180–260 °C [31,33,63,65–74].

The dry torrefaction process is a thermochemical method taking place at 200–300 °C, usually in an inert atmosphere, for 30–60 min. It is also known as mild pyrolysis [75], low-temperature pyrolysis [76], or thermal annealing [77,78]. In the case of the non-oxidative torrefaction [52,53,79], N_2 [20,62,80] and CO_2 [20,81] are commonly used as carrier gases; while CO_2 is usually used as a carrier gas to move lignocellulosic particles during thermal treatment. In the case of oxidative torrefaction [50,51,82], air [79], flue gas [83], and other O_2-containing gases [82,84] were used as carrier gases to move the feeding material particles. Oxidative torrefaction is faster compared to the non-oxidative one because of the existence of O_2 and the thermal degradation exothermic reactions taking place during the torrefaction process [82,85,86]. The use of air or flue gas as carrier gases reduces operating costs for nitrogen removal, necessary in the case of non-oxidative torrefaction, and produces fuels with similar properties. In addition, the solid yield in the case of oxidative torrefaction is decreased compared to that of the non-oxidative one [82,84,87,88]. Finally, the higher heating value (HHV) of the product was found to decrease in the case of an O_2 concentration increase [87,89].

2.2. Wet Torrefaction

Wet torrefaction [60,90–92] is a different torrefaction process compared to dry torrefaction. In this process, the lignocellulosic feedstock is treated using subcritical water at 180–260 °C, for 5–240 min, and pressures of up to 5 MPa, [30,79,81,93–95]. The wet torrefaction process can produce liquid and solid fuel. Wet torrefaction is also known as hydrothermal carbonization [18,40,96–99], hydrothermal torrefaction [58,100,101], hot water extraction [102], autohydrolysis [103–105], hydrothermolysis [106–109], hot compressed water treatment [91,94], water hydrolysis [110], aqueous fractionation [101], solvolysis/aquasolv [106], aqueous liquefaction [110,111], or pressure cooking [92,112]. Moreover, acid-catalyzed wet torrefaction [54] can be achieved using acids [113], such as H_2SO_4 and acetic acid, or salts such as LiCl [60,113]. The use of such catalysts facilitates the wet torrefaction process comparably to the dilute acid hydrolysis process [114–116]. Wet torrefaction requires lower temperatures compared to dry torrefaction. Lignocellulosic biomass type, feedstock particle size distribution, reaction temperature, reaction time, catalyst concentration, and solid-to-liquid ratio affect the product type and properties. The lignocellulosic feedstock hemicelluloses are hydrolyzed producing monosaccharides and oligosaccharides as regards the liquid phase, while the solid phase product is lignin-rich biochar with low humidity [117,118]. The liquid phase chemicals must be treated/recycled to avoid environmental damage, while monosaccharides and oligosaccharides produced in the liquid phase, possess high values without environmental damage [58,97,98,100,101].

The properties of the water used for wet torrefaction, e.g., density, viscosity, dielectric constant, ion products, and diffusivity, change significantly affecting the lignocellulose degradation [30]. Consequently, wet torrefaction is usually conducted under a near-subcritical state. Hot compressed water degraded lignocellulosic feedstock produces volatile acids [90], facilitating the depolymerization process [119]. Monosaccharides, such as glucose, xylose, mannose, and arabinose, formed in the liquid phase, can be used for bioethanol production. Additionally, wet torrefaction can achieve a similar solid product with high HHV under much lower temperatures compared with dry torrefaction [113,120]. Moreover, energy-consuming pre-drying is not necessary in wet torrefaction as in dry torrefaction. The ash content of wet torrefaction pretreated lignocellulose is reduced compared to dry torrefaction assigned to the ash minerals dissolution into the aqueous phase preventing problems such as corrosion, deposition, agglomeration, slagging, and fouling, during the product's further processing [121,122].

2.3. Steam Torrefaction

Steam torrefaction uses high temperature/pressure steam explosion to swell the cellulosic fibers and makes the lignocellulosic complex more open for the next step processes, i.e., hydrolysis, fermentation, or densification [123,124]. Steam torrefaction improves the recovery of monosaccharides and oligosaccharides of lignocellulosics fermentable to bioethanol [124]. Steam torrefaction uses high-pressure/temperature steam in a sealed chamber with lignocellulosic feedstock at 200–260 °C for 5–10 min. The steam torrefaction uses lower temperatures/times compared to the dry one [125,126]. The pressure is rapidly released causing swelling of the lignocellulosic matrix and separation of the cellulosic fibers [125,127,128]. The feedstock's low molecular weight volatiles are eliminated during the process, improving the product's HHV and carbon content, simultaneously decreasing the particle size distribution, humidity, hydrophobicity elasticity, mechanical strength, and bulk density [125,129,130]. Steam torrefaction needs no carrier gas like dry torrefaction. The properties of the solid products make them appropriate for manufacturing pellets [125,126,129,130].

2.4. Microwave-Assisted Torrefaction

Microwave-assisted torrefaction uses microwave heating instead of conventional heating [46,48,122,131]. Microwave achieves low energy consumption, and fast internal and volumetric heating, of the lignocellulosic feedstock [55,59,61,113,116,132]. The microwave-assisted torrefaction operating condition, power level, energy efficiency, types of absorbers/catalysts, and feedstock's particle size distribution substantially affects the product's properties as regards HHV, energy/mass yields, mass loss, fuel ratio, H/C ratio, and O/C ratio. Finally, MWT has the capacity to serve as a technique to improve the performance of the feedstock [7,47,49,56,57,133–137]. The classification of the various torrefaction processes is shown in Figure 1, according to the relevant literature [3,138].

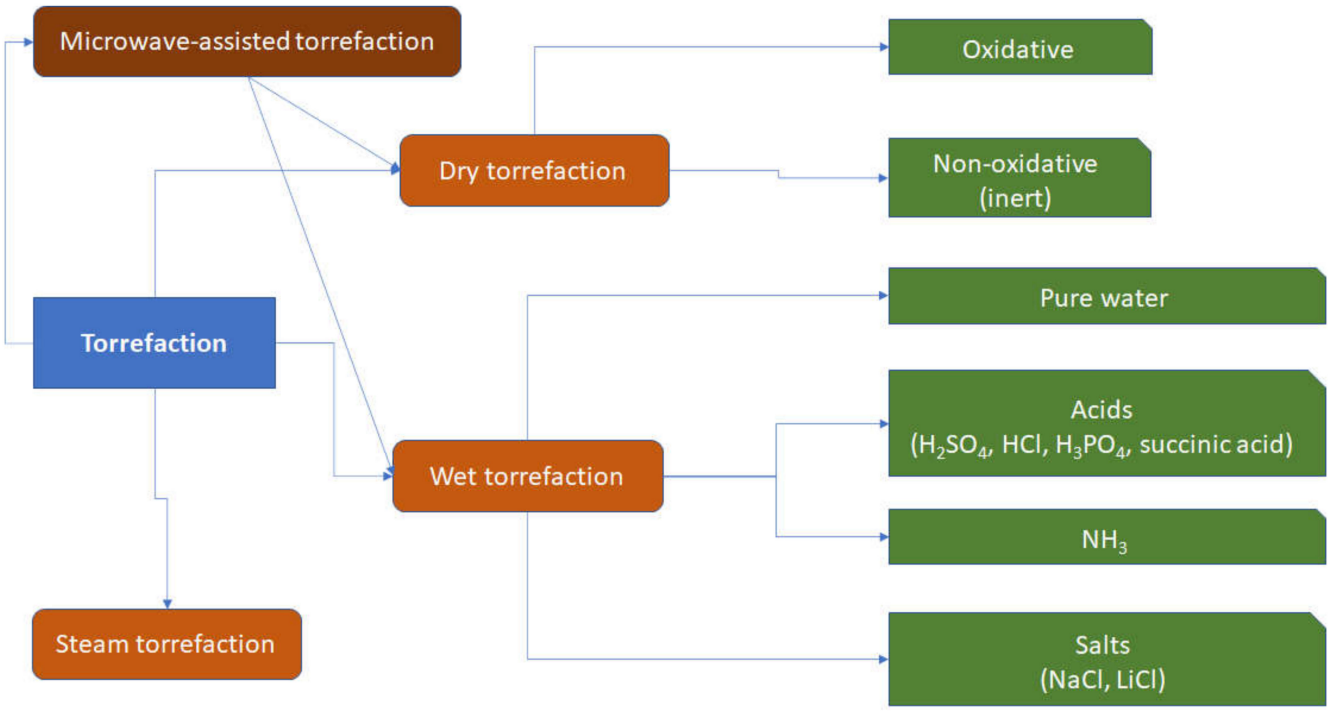

Figure 1. Classification of torrefaction.

3. Torrefaction Reactors

Torrefaction reactors can be separated into those with (i) indirect and (ii) direct heating systems [3,139]. The reactors with the indirect heating system could be separated into (a) rotary and (b) screw (auger) reactors. Additionally, the reactors with the direct heating system could be separated into those in which the heating medium (a) does not contain oxygen, and (b) contains a small amount of oxygen [3,138–142]. Machines with screw/belt conveyors, rotary, vibrating, microwave, stepped, and moving beds are used as torrefaction reactors [3]. The most used types of reactors are the rotary drum, the microwave, and the fixed/fluidized and horizontal/vertical moving bed [1,139,142]. Moreover, many other reactors are used, e.g., the belt drier, the spouted bed reactor, the rotating-packed bed reactor, the vibrating electrical elevator, the multiple hearth furnace, and the torbed reactor [5,138,143–148]. The classification of the torrefaction reactors based on the international literature [3,138–142] is presented in Figure 2.

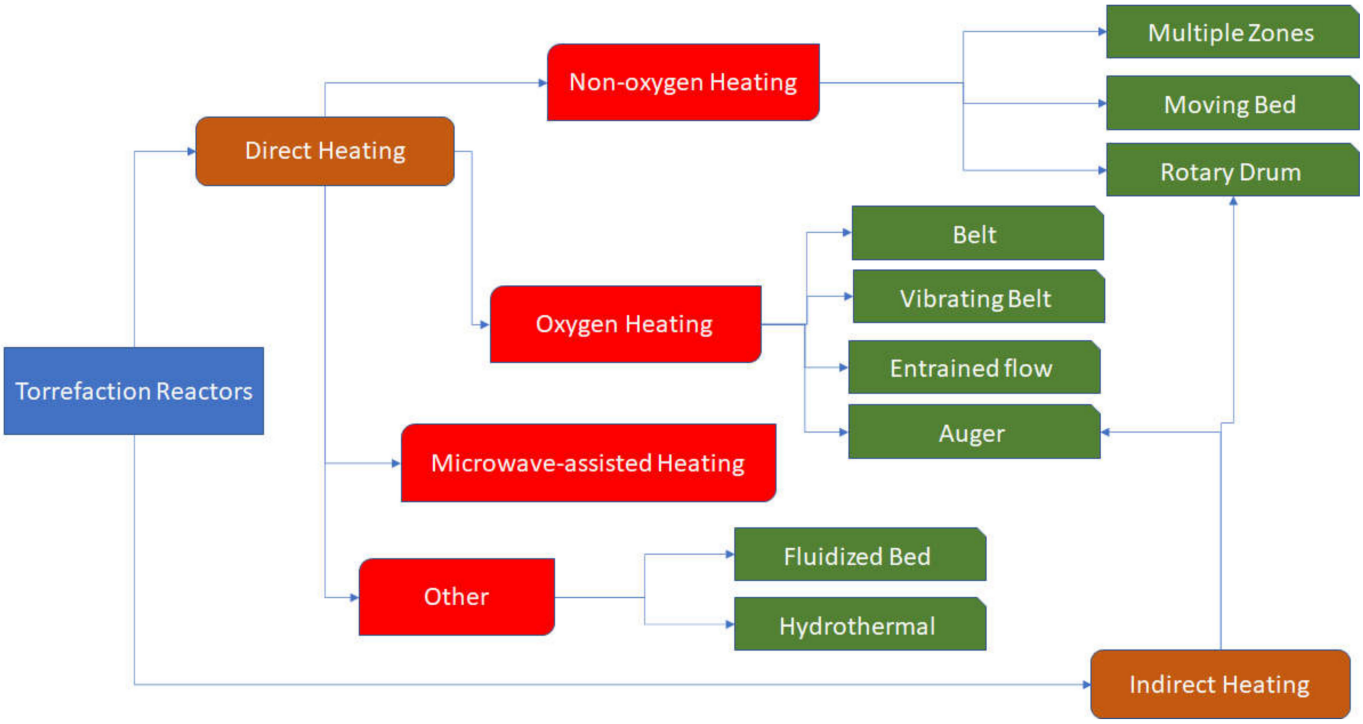

Figure 2. Torrefaction reactors classification.

4. The Torrefaction Conditions Effect on the Lignocellulosic Biomass Characteristics

4.1. The Torrefaction Conditions Effect on the Lignocellulosic Feedstock Composition: Cellulose, Hemicelluloses, and Lignin

The torrefaction conditions effect on the lignocellulosic biomass composition, i.e., cellulose, hemicelluloses, and lignin are presented in Table 1 as regards dry torrefaction and in Table 2 as regards wet torrefaction processes according to various researchers. The hemicellulose percentage decreases more easily than that of the cellulose one because of the amorphous structure and the lower degree of polymerization of hemicelluloses [149]. The cellulose percentage decreases less easily because the thermal cracking of cellulosic chains is not easy as they are long and have highly organized crystalline structures [150–152]. The lignin percentage increases by torrefaction treatment compared to the raw (untreated) lignocellulosic materials due to the development of low molecular weight lignin accumulated on the material surface at moderate treatment conditions [150]. Herbaceous lignocellulosic materials, such as agricultural crop residues and grasses, depolymerize easier compared to woody biomass [153]. Deciduous woods hemicelluloses consisting mostly of xylan decompose easier than coniferous wood glucomannan [27]. Glucomannan requires relatively higher temperatures to degrade compared to xylan. Cellulose devolatilizes at 200–400 °C, hemicelluloses at 100–290 °C, and lignin at over 400 °C [29,85]. Torrefaction starts with dehydration and removes lighter volatiles. Hemicelluloses and amorphous cellulose start to depolymerize first by fragmentation, deacetylation, and depolymerization, while crystalline cellulose requires more severe conditions. Hemicellulose fragmentation produces acetic acid and formic acid. Lignin decomposes with difficulty because of its complex matrix. Cellulose and hemicellulose's thermal cracking during torrefaction is more extended compared to that of lignin. Torrefaction devolatilizes, dehydrates, decarboxylates, and decarbonylates the lignocellulosic feedstock [89,154].

Table 1. Raw and dry-torrefied lignocellulosic biomass composition.

Biomass	Raw/ Torrefied	Temperature (°C)	Time (min)	Cellulose	Hemicelluloses	Lignin	References
Bamboo	Raw	-	-	34.1	27.7	24	[150]
Bark of Douglas fir	Raw	-	-	25.4	8.1	51	
Cherry wood samples	Raw	-	30	42.8	24.3	32.9	[25]
	Torrefied	350	30	6.8	0.0	93.2	
Coconut fiber	Raw	-	-	47.10	12.50	31.35	[79]
Cotton stalk	Raw	-	-	34.81	17.46	18.92	[155]
	Torrefied	257.8	60	31.62	2.44	54.49	
Cryptomeria japonica	Raw	-	-	43.60	16.01	32.20	[79]
Douglas fir	Raw	-	-	42.5	17.9	22	[150]
Eucalyptus	Raw	-	-	48.36	15.35	21.26	[79]
Groundnut stalks	Raw	-	-	36.28	32.4	20.12	[36]
	Torrefied	250	120	39.5	26.5	20.6	
Hops (*Humulus lupulus*)	Raw	-	-	42.2	-	26.2	[156]
	Torrefied	250		47.0	-	35.1	
Miscanthus (*Miscanthus* × *giganteus*)	Raw	-	-	41.4	19.7	22.6	
	Torrefied	250	90	44.1	8.4	41.6	
Mixed waste wood	Raw	-	90	37.2	23.8	27.0	
	Torrefied	250		42.8	16.7	32.9	
Oak waste wood	Raw	-	-	38.3	25.5	22.0	
	Torrefied	250	90	43.7	7.7	31.4	
Oil palm fiber	Raw	-	-	26.78	34.00	16.08	[79]
Sugarcane bagasse	Raw	-	-	23.08	18.81	11.35	[53]
	Torrefied	250	60	22.46	7.21	57.32	
Sugarcane leaves	Raw	-	-	41.41	36.68	6.39	[41]
	Torrefied	275	-	46.06	4.01	36.53	
Tobacco rod	Raw	-	-	31.28	13.65	22.37	[65]
	Torrefied	240	30	1.28	0.00	77.22	
Vine pruning	Raw	-	-	37.60	19.23	15.77	[155]
	Torrefied	275	20	35.04	3.01	56.82	
Wheat straw	Raw	-	-	37.40	22.88	29.30	[36]
	Torrefied	250	120	41.55	16.40	29.95	
Wood dust biomass sourced	Raw	-	-	34.50	26.50	30.0	[157]
	Torrefied	250	45	40.0	3.5	52.0	

Especially, according to Table 1, as regards dry-torrefied Miscanthus (*Miscanthus* × *giganteus*), mixed waste wood, oak waste wood [156], sugarcane leaves [41], and wheat straw [36], an increase in cellulose percentage of about 3–5 units compared to the raw materials was observed. On the contrary, as regards their hemicelluloses percentages, a significant reduction of up to 18 units was presented. Simultaneously, the lignin percentage of the dry-torrefied materials significantly increases in relation to the untreated ones. Similar observations can be made regarding the materials that have undergone wet torrefaction. In

general, dry-torrefied biomass shows higher insoluble lignin content than wet-torrefied biomass. Finally, dry-torrefied materials show a higher increase in cellulose and a decrease in hemicelluloses compared to the wet-torrefied feedstock.

Table 2. Effect of wet torrefaction on the lignocellulosic biomass composition.

Biomass	Raw/Torrefied	Temperature (°C)	Time (min)	Cellulose	Hemicelluloses	Lignin	References
Corn stalk	Raw	-	-	29.08	25.99	15.04	[61]
	Torrefied (Microwave)	180	30	37.33	18.82	19.61	
	Torrefied (Microwave, NH_3)	180	-	30	40.59	19.86	
Corncobs	Raw	-	-	34.490	35.36	-	[158]
	Torrefied	185	5	54.11	20.05	-	
Tobacco rod	Raw	-	-	31.28	13.65	22.37	[65]
	Torrefied	240	30	1.28	0.0	77.22	

4.2. Torrefaction Conditions Effect on the Lignocellulosic Biomass Proximate and Ultimate Analysis Results

The torrefaction conditions' effect on the lignocellulosic feedstock proximate and ultimate analysis results is presented in Table 3 as regards dry torrefaction and in Table 4 as regards wet torrefaction. Fixed carbon, volatile matter, moisture, and ash were determined using proximate analysis for various kinds of raw and torrefied lignocellulosic materials by numerous researchers. The ultimate analysis results as regards carbon, hydrogen, oxygen, and nitrogen percentages, are also presented in these Tables 3 and 4. The proximate analysis results changes due to the degradation of the lignocellulosic material's oxygen-containing functional groups [159]. The raw feedstock has a lower fixed carbon percentage and higher volatile matter percentage compared to the torrefied material. Dehydration decreases moisture percentage while dehydration, depolymerization, and fractionation reactions decrease volatile matter percentage during the torrefaction process. Ash, i.e., inorganic mineral matter, catalyzes the removal of volatile matter during torrefaction. Moreover, ash percentage affects the torrefied product's yield and composition and increases slightly by torrefaction severity increasing [160].

Table 3. Lignocellulosic biomass proximate and ultimate analysis results before and after dry torrefaction.

Biomass	Raw/ Torrefied	Temperature (°C)	Time (min)	Proximate Analysis (wt.%)				Ultimate Analysis (wt.%)				Reference
				Moisture	Volatile Matter	Fixed Carbon	Ash	C	H	O	N	
Rice straw	Raw				76.56	14.02	9.48	39.61	5.83	43.80	1.21	[161]
	Torrefied	300	-	-	52.00	32.70	15.31	49.90	4.61	28.43	1.77	
Rice husk	Raw	-	-	-	70.41	15.79	13.80	38.62	5.67	41.38	0.48	[161]
	Torrefied	300	-	-	51.42	28.91	19.68	46.43	4.60	28.91	0.58	
Coffee husk	Raw	-	-	2.7	77.7	17.9	1.7	48.5	5.9	40.6	2.8	[162]
	Torrefied	300	60	1.4	63.5	31.8	3.3	61.2	4.8	15.3	3.5	
Spent coffee grounds	Raw	-	-	3.3	81.2	14.6	0.9	50	6.7	39	2.3	[162]
	Torrefied	300	60	1.2	67.8	29	2	69.5	6	19	3.2	
Wheat straw	Raw	-	-	7.33	65.43	16.20	11.04	49.3	5.18	44.66	0.80	[36]
	Torrefied	500 °C/ min	-	2.50	58.57	23.90	14.90	53.90	4.90	40.82	0.67	
Groundnut stalks	Raw	-	-	3.78	74.83	16.70	4.69	34.52	9.80	51.50	1.16	[36]
	Torrefied	500 °C/ min	-	2.0	70.86	19.68	21.59	41.20	8.70	47.70	1.19	
Rice husk	Raw	-	-	7.44	56.13	20.45	15.98	42.39	5.77	50.10	1.17	[51]
	Torrefied	300	-	4.63	14.13	38.09	43.15	70.84	3.07	24.49	1.55	
Miscanthus	Raw	-	-	9.2	83.9	3.9	2.9	46.2	3.9	45	0.8	[156]
	Torrefied	300	-	4.8	56	25.4	6	50.6	4.2	34.5	4.2	
Hops (*Humulus lupulus*)	Raw	-	-	11.8	82.9	1.9	3.3	42.3	4.8	36.8	2.4	[156]
	Torrefied	300	-	9.8	66.7	14.4	8.9	46.3	4.1	22.6	2.8	
Mixed waste wood	Raw	-	-	8.9	78.4	9.5	3.1	46.5	5.5	44.3	0.4	[156]
	Torrefied	300	-	4.7	65.3	23.1	6.8	57.8	2.2	32.3	0.6	
Oak waste wood	Raw	-	-	7.9	80.4	11.1	0.6	46.9	5.9	46.1	0.3	[156]
	Torrefied	300	-	5.5	62.4	27.3	4.9	60.8	3.2	32.5	0.5	

Table 3. *Cont.*

Biomass	Raw/ Torrefied	Temperature (°C)	Time (min)	Proximate Analysis (wt.%)				Ultimate Analysis (wt.%)				Reference
				Moisture	Volatile Matter	Fixed Carbon	Ash	C	H	O	N	
Sugarcane bagasse	Raw	-	-	-	83.46	14.26	2.17	46.37	6.29	46.79	0.55	[53]
	Torrefied	275	60	-	51.85	44.04	3.95	58.25	2.81	38.68	0.31	
Wood pellet	Raw	-	-	5.42	84.72	15.07	0.22	47.48	6.47	45.94	0.09	[113]
	Torrefied	275	60	-	73.21	26.38	0.41	53.97	5.87	40.01	0.12	
Barley straw	Raw	-	-	6	74.3	-	8.4	45.5	5.5	47.9	0.99	[163]
	Torrefied	300	37.5	3.5	62.5	-	16.1	57.5	4.1	36.4	1.6	
Corn straw	Raw	-	-	6.18	71.21	16.12	6.49	45.84	5.11	34.89	1.28	[164]
	Torrefied	325	-	3.02	53.23	34.73	9.02	53.84	4.12	27.57	2.36	
Empty fruit bunches	Raw	-	-	4.55	77.42	13.84	4.19	42.82	6.07	50.57	0.54	[165]
	Torrefied	300	-	2.21	49.85	38.05	9.89	58.89	5.12	34.83	1.16	
Rubberwood sawdust (RWS)	Raw	-	-	4.60	81.80	16.60	1.61	48.67	6.03	43.48	0.09	[166]
	Torrefied	300	40	0.73	43.75	52.42	3.83	69.41	4.85	21.49	0.36	
Cotton stalk	Raw	-	-	6.15	75.35	21.57	5.08	47.91	5.66	45.57	0.75	[155]
	Torrefied	257.8	60	-	58.27	34.28	6.45	61.23	4.69	33.16	0.85	
Vine pruning	Raw	-	-	6.84	72.12	23.68	4.2	49.28	5.53	44.21	0.84	[155]
	Torrefied	275	20	-	59.96	34.91	5.13	62.20	4.09	32.63	0.98	
Wheat straw	Raw	-	-	4.1	76.4	17.3	6.3	47.3	6.8	37.7	0.8	[76]
	Torrefied	290	-	0.8	51.8	38	19.2	56.4	5.6	27.6	1.0	
Willow	Raw	-	-	2.8	87.6	10.7	1.7	49.9	6.5	39.9	0.2	[76]
	Torrefied	290	-	0.0	77.2	20.5	2.3	54.7	6	36.4	0.1	

Table 4. The wet torrefaction effect on the proximate and ultimate compositions of lignocellulosic feedstock.

Biomass	Raw/ Torrefied	Temperature (°C)	Catalyst	Time (min)	Proximate Analysis (wt.%)				Ultimate Analysis (wt.%)				Reference
					Moisture	Volatile Matter	Fixed Carbon	Ash	C	H	O	N	
Bamboo Saw dust	Raw	-	-	-	10.1	74.9	9.2	5.8	46.73	6.18	47.66	0	[69]
	Torrefied	140	Acid	30	4.5	66	30	0.3	51.4	6.5	42.04	0.02	
Orange peel	Raw	-	-	-	-	74.85	12.47	2.8	45.1	8.78	42.3	0.46	[68]
	Torrefied	280	No	30	-	58.28	34.46	7.26	58.32	6.62	30.46	0.24	
Barley straw	Raw	-	-	-	6.00	74.30	17.3	8.40	45.53	5.50	47.86	0.99	[54]
	Torrefied	200	Acid	25	5.10	72.30	27.2	5.5	52.51	5.79	40.71	0.85	
Grass	Raw		-	-	-	72.33	12.2	9.3	45.6	6.4	46.4	1.6	[167]
	Torrefied	200	No	60	-	63.5	27.5	6.26	56.1	5.9	36.6	1.4	
Miscanthus	Raw		-	-	8.18	65.43	14.22	12.17	43.3	5.86	37.54	1.12	[168]
	Torrefied	200	acid	-	5.76	68.14	21.39	4.71	53.75	5.62	33.82	0.21	
Palm kernel shell	Raw	-	-	-	4.5	68.5	22.5	4.6	47.9	6.1	40.7	0.52	[169]
	Torrefied	220	No	30	1.3	67.6	29.2	2.0	55.9	5.6	36.1	0.40	
Spruce	Raw	–	-	-	-	86.50	13.27	0.23	50.31	6.24	43.38	0.07	[121]
	Torrefied	225	No	30	-	74.74	25.12	0.14	56.99	5.87	37.07	0.07	
Birch	Raw	-	-	-	-	89.46	10.26	0.28	48.94	6.35	44.60	0.11	[121]
	Torrefied	225	No	30	-	73.78	26.09	0.13	56.92	5.86	37.13	0.09	
Adansonia digitate (Baobab)	Raw	-	-	-	11.93	61.23	23.61	3.23	43.16	5.78	50.47	0.54	[170]
	Torrefied	250	No	120	2.17	53.98	36.76	7.09	46.03	4.11	49.45	0.39	
Corn stalk	Raw	-	-	-	-	87.19	2.59	2.59	44.49	6.25	46.37	0.30	[171]
	Torrefied	220	No	30	-	79.56	19.99	0.45	53.25	5.99	39.95	0.36	
Microalgae (*Chlorella vulgaris* ESP-31)	Raw	-	-	-	-	74.59	16.39	9.02	53.01	8.67	35.05	3.26	[122]
	Torrefied	170	No	30	-	67.70	25.76	6.54	59.03	7.82	24.53	8.62	
Spruce	Raw	-	-	-	-	86.50	13.27	0.23	50.31	6.24	43.38	0.07	[172]
	Torrefied	222	No	5	-	81.51	18.39	0.10	55.75	6.05	38.14	0.06	
Olive tree pruning	Raw	-	-	-	6.2	79.91	17.31	2.78	48.15	5.74	45.67	0.39	[173]
	Torrefied	280	No	360	2.91	42.33	55.48	2.18	74.86	4.88	19.04	1.18	

The results in Tables 3 and 4 show that the ash percentage decreases via wet torrefaction. Different results were provided for orange peel and Adansonia digitata (Baobab) trunk in which the increase in temperature produced higher ash and fixed carbon percentages for both types of biochar. However, the percentage of volatile matter decreased by increasing torrefaction temperature [68]. The reduction could be a result of the passing of inorganic carbonates and mineral oxides from the solid to the liquid phase [167]. In contrast, in dry torrefaction, an increase in ash percentage was observed due to the breakdown of the aforementioned inorganic carbonates and oxides from the solid phase minerals. The low ash content of biomass is advantageous in terms of fuel properties. Higher ash content can cause fouling, aggregation, and reduced heat transfer [36].

As regards ultimate analysis results presented herein, the oxygen and hydrogen percentage of the lignocellulosic feedstock significantly decreases during torrefaction, increasing the carbon percentage and consequently enhancing the energy content of the product. The release of volatile matter, moisture, and gases such as CO_2, CO, CH_4, and H_2, reduces the oxygen and hydrogen percentages of the torrefied materials simultaneously increasing the fixed carbon percentage [174]. A significant decrease in hydrogen percentage was observed as regards the dry torrefaction, while a high-level decrease in oxygen percentage was observed for wet torrefaction. The carbon percentage increased mainly in the case of wet torrefaction. The nitrogen percentage decreased as regards the wet torrefaction but increased for the dry torrefaction. The results revealed a significant change in carbon percentage after torrefaction. A reduction in the volatile matter was noticed in both torrefaction types, with the greatest reduction found in dry torrefaction. Furthermore, both torrefaction types resulted in an increase in fixed carbon percentage. The change in the percentage of volatile matter and fixed carbon content in the torrefied biomass compared to the raw one was due to the carbonization of the carbohydrates during torrefaction which further enhances the carbon content. Finally, it was found that through the torrefaction process, biomass releases water and decomposes the reactive hemicellulosic fraction, causing a volatiles decrease in combination with a calorific value increase.

The carbohydrate cracking and the volatiles release take place due to decarboxylation and dehydration reactions at high treatment temperatures [142]. The severe torrefied biomass composition is relatively like that of lignite, peat, and coal [152].

4.3. The Torrefaction Conditions Effect on the Higher Heating Value, Energy Yield and Density, and Mass Yield of the Lignocellulosic Feedstock

The torrefaction conditions' effects on the HHV, energy yield, mass yield, and energy density of the lignocellulosic materials are given in Table 5 for the case of dry torrefaction and in Table 6 for wet torrefaction. The mass yield is defined as the ratio of the weight of the torrefied material to the raw material weight. Volatile matter and moisture decrease, in combination with the devolatilization and thermal cracking of hemicelluloses, cellulose, and lignin, leads to weight reduction during the torrefaction process [175]. Combined rod-milling and torrefaction pretreatment considerably increased carbon percentage and HHV, proving that rod-milling as the first step in the torrefaction process is a factor that has a positive effect on torrefaction's efficiency. This weight reduction is mostly due to the hemicelluloses' degradation. The solid residue mass yield changes by the torrefaction conditions severity. The agricultural feedstock mass yield is lower compared to that of woody biomass because agricultural biomass has higher hemicelluloses percentage [176]. The behavior of cellulose, hemicelluloses, and lignin differs during torrefaction pretreatment. Hemicelluloses react easier with oxygen-producing liquid and gaseous products while carbon stays in the solid phase resulting in higher HHV. Thermogravimetric analysis (TGA) showed that the weight reduction is due to the devolatilization and the hemicelluloses, cellulose, and lignin degradation. The product distribution from various torrefaction technologies includes (i) solid, (ii) water (thermal decomposition reaction water and evaporation released freely bound water), condensable volatile organic compounds (acetic acid, alcohols, aldehydes, ketones, C_xH_y, toluene, ben-

zene), and lipids (fatty acids, waxes), and (iii) non-condensable gases (CO_2, CO, CH_4). The main products are char, gases, and condensable liquid/tar. The percentage of each product depends on the torrefaction parameters (temperature, heating rate, time), and on the feedstock characteristics. Usually, solid is approximately 70% while gases and tar are 30% [177,178]. In the case of lignocellulosic biomass and microalgae co-torrefaction, biochar was 23–90%, the aqueous phase was 1–58%, bio-oil was 0–36%, and gas was 1–25%, depending on the torrefaction severity [179]. Torrefaction increases the HHV of the product depending on the pretreatment severity [177]. Generally, higher torrefaction severity gives desirable results such as enhanced product's HHV but not without any cost since it also gives low mass yield. The increased fixed carbon percentage and the decreased oxygen percentage increase the product's HHV and energy density. Energy density is the energy in a volume unit of the material under examination. Moreover, the energy yield is defined as the ratio of the torrefied feedstock's energy content to that of the raw material. Torrefaction severity increases the energy content but decreases the mass yield of the product, resulting in a decrease in the energy yield. Torrefaction severity increases HHV but decreases mass yield. Microwave torrefaction enhances the mass/energy yields of the wheat straw [36,76,175,178–181], barley straw [57,134,163], rice straw [136,161,182], rice husk [51,159,161,183–186], canola hull [12], fir [125,129,130,137,187], grass [167], and sugarcane residue [41,53,113,116,188]. Good results were reported for wood sawdust torrefaction using a continuous spouted bed reactor [168].

Table 5. Raw and dry-torrefied lignocellulosic feedstock's high heating value, mass yield, energy yield, and energy density.

Biomass	Raw/ Torrefied	Temperature (°C)	Time (min)	HHV (MJ/kg)	Energy Yield (%)	Mass Yield (%)	Energy Density	Reference
River tamarind	Raw	-	-	17.9			1	[189]
	Torrefied	300	25	21	44.3	34.2	1.3	
Sawdust	Raw			18.9			1	[82]
	Torrefied	290	7	21.8	73.8	-	1.15	
Spruce	Raw			18.3			1	[190]
	Torrefied	280	52	21.5	84	76	1.17	
Mustard stalk	Raw	-	-	16.9				[191]
	Torrefied	300	20	21.3	81.3	64.5	N/A	
Pepper stem/coffee grounds pellets	Raw	-		16.5				[192]
	Torrefied	250	30	21.5	87	83.6	N/A	
Sugarcane leaves	Raw			17.7				[41]
	Torrefied	275	30	20.1	70	67.9	N/A	
Wheat straw	Raw			17.5			1	[175]
	Torrefied	300	30	22.5	64	49.7	1.29	
Wheat straw	Raw			18.9			1	[76]
	Torrefied	290	30	22.6	65.8	55	1.2	
Microalgae/ lignocellulosic biomass	Raw	-		N/A				[179]
	Torrefied	300	60	19.3	40.8	78	N/A	
Coal/sugarcane bagasse	Raw	-		18.73			1	[193]
	Torrefied	300	45	25.83	74.7	54.1	1.38	
Coal/corn cob	Raw			18			1	[193]
	Torrefied	300	45	24.31	76.5	56.7	1.35	
Coal/pine saw dust	Raw			20			1	[193]
	Torrefied	300	45	28.27	74	52.44	1.41	

Table 5. *Cont.*

Biomass	Raw/ Torrefied	Temperature (°C)	Time (min)	HHV (MJ/kg)	Energy Yield (%)	Mass Yield (%)	Energy Density	Reference
Wheat straw	Raw			18.2			1	[181]
	Torrefied	250	360	20.8	77.1	61.2	1.14	
Wheat straw	Raw			19.2			1	[151]
	Torrefied	250	30	20.9	41.2	51.1	1.15	
Corn cob	Raw			14			1	[194]
	Torrefied	250	60	21	110	68	1.55	
Rice husk	Raw			15.5			1	[194]
	Torrefied	275	60	19.5	95	75	1.2	

Table 6. Raw and wet-torrefied lignocellulosic feedstock's high heating value, and mass/energy yield.

Biomass	Raw/ Torrefied	Temperature (°C)	Time (min)	Catalyst	HHV (MJ/kg)	Energy Yield (%)	Mass Yield (%)	Reference
Spruce	Raw				20.4			[172]
	Torrefied	222	5	None	22.6	N/A	74.1	
Barley straw	Raw				17.5			[54]
	Torrefied	200	25	Acid	24.3	68	31	
Dewatered poultry sludge	Raw				26.6			[42]
	Torrefied	268	47	None	28.6	N/A	85.2	
Palm kernel shell	Raw				18.9			[169]
	Torrefied	220	30	None	23.4	N/A	47.2	
Microalgae	Raw				20.8			[55]
	Torrefied	160	10	H_2SO_4	32.2	43	15	

Table 6. *Cont.*

Biomass	Raw/ Torrefied	Temperature (°C)	Time (min)	Catalyst	HHV (MJ/kg)	Energy Yield (%)	Mass Yield (%)	Reference
Tobacco stalk	Raw				13.8			[19]
	Torrefied	240	60	None	22.8	N/A	41.8	
Spruce	Raw				20.4			[121]
	Torrefied	225	30	None	23	N/A	69.7	
Birch	Raw				19.9			[121]
	Torrefied	225	30	None	22.9	N/A	58	[121]
Rice husk	Raw				16.2			[159]
	Torrefied	240	60	None	18.1	52	48	
Almond-tree pruning	Raw				17.6			[195]
	Torrefied	N/A	N/A	None	24	77	57.1	
Microalgae	Raw				N/A			[122]
	Torrefied	170	30	None	26	63	55	
Miscanthus	Raw				18.8			[196]
	Torrefied	220	10	None	20.1	75	70	
Yard waste	Raw				15.6			[72]
	Torrefied	220	30	None	23.6	65.8	43.5	
Sugarcane leaves	Raw				17.7			[41]
	Torrefied	250	30	None	23.3	43	34.5	

5. Simulation and Optimization of the Lignocellulosic Biomass Torrefaction Process

5.1. Simulation of the Lignocellulosic Biomass Dry Torrefaction Process

5.1.1. Artificial Neural Network Approaches

Multivariate adaptive regression splines (MARS) in combination with artificial neural networks (ANN) are two useful tools in artificial intelligence (AI), a machine learning (ML) type, for complex data pattern analysis [4,197,198]. The torrefaction severity index (TSI) compromises the different torrefaction conditions' effect on the quality of the torrefied lignocellulosic biomass. Chen et al. [197], used the ANN approach in combination with MARS models to simulate the torrefaction process and forecast the TSI. Lignocellulosic feedstock type, torrefaction temperature, and time were the input simulation parameters for the ANN and MARS approaches. Temperature was the most influential factor in TSI forecasting using the MARS model, followed by reaction time and lignocellulosic biomass type. On the contrary, feedstock type is the dominant factor according to the ANN approach, while temperature and time effect on TSI is not significant. Three different combinations of numbers of neurons and hidden layers were used for the ANN evaluation. It was found the two hidden layers in combination with 85 neurons gave the optimum performance. Good fitting was achieved for both ANN and MARS models using relative root means square error analysis. The MARS model had a better fit as regards solid biofuel's TSI, while the input parameter sensitivity of the ANN model was lower. The number of neurons and hidden layers significantly affect the ANN model performance.

García Nieto et al. [198] introduced a new support vector machines (SVMs) hybrid algorithm, with the optimization method of simulated annealing (SA), for HHV value of torrefied feedstock forecasting incorporating the torrefaction process experimental operation input parameters. They used the MARS approach in combination with the technique of random forest (RF). The model predicted sufficiently the significance of each physical–chemical variable on the HHV. It was compared with several HHV forecasting models. This hybrid SVM–SA-based model with RBF kernel function successfully fitted the set of experimental data with the optimal hyperparameters. The findings fitted better with the experimental data than those obtained by the RF–SA-based technique and the MARS–SA-based approach.

Moreover, this research group formed a new hybrid algorithm, with SVMs and particle swarm optimization (PSO) method, for forecasting the lignocellulosic feedstock's HHV from experimental torrefaction operation input parameters [199]. Furthermore, RF in combination with a multilayer perceptron network (MLP) successfully fitted the experimental data. The physical–chemical parameters of this industrial process were monitored and analyzed. The significance of each physical–chemical variable on the HHV was satisfactorily simulated according to the model. The hybrid PSO–SVM-based approach with cubic kernel function successfully fitted the experimental dataset and correlated with the optimal hyperparameters. The PSO–SVM-based model gave better results than the MLP approach and RF-based model. In addition, a two-stage reaction model (TSR) in combination with a PSO algorithm was developed to forecast the isothermal reaction kinetics of thermal degradation of hemicelluloses, cellulose, and lignin during this process for biochar production [32].

5.1.2. Kinetic and Thermodynamic/Thermochemical Approaches

Several kinetic models have been established on the three main components of lignocellulosic biomass (cellulose, hemicelluloses, and lignin), appropriate to describe the thermochemical decomposition mechanisms as regards the torrefaction process. Di Blasi and Lanzetta [200] established a two-step kinetic model for the investigation of the xylan degradation isothermal kinetics during pyrolysis. The activation energies of the first and second steps were 76.57 kJ/mol and 54.81 kJ/mol, respectively. They assumed that the degradation takes place under kinetic control and that a semi-global reaction mechanism is valid. Prins et al. [201] applied this two-step, first-order mechanism to simulate the solid yield reduction in the case of kinetically controlled torrefaction of willow. Furthermore, multi-step kinetic models were applied to torrefaction to forecast reaction rates and product

yields. Onsree et al. [202], applied a two-step kinetic model assuming that the biomass decomposition mechanism through torrefaction consisted of serial primary and secondary reactions. Volatiles and solid intermediates were formed during the first step, while other volatiles and chars were formed due to the decomposition of these intermediates during the second step. Similarly, a two-step first-order reaction mechanism was proposed by Ikegwu et al. [203] to simulate the torrefaction of pine sawdust. MATLAB software (Mathworks, Natick, MA, USA) was used for the kinetic analysis and the solid/gas product distribution according to the reaction mechanism. Soria-Verdugo et al. [204] found that inert torrefaction can be simulated using a two-step reaction mechanism, but a three-step reaction mechanism is required for oxidative torrefaction. They used a model-fitting kinetics method on non-isothermal torrefaction data. The three-step mechanism was appropriate for both isothermal and non-isothermal torrefaction simulation. The two-step first-order kinetic model accepts that raw biomass, decomposes into an intermediate solid, by freeing moisture and volatiles. The intermediate solid is then decomposed into a solid residue and more volatile matter is produced. The extended two-step first-order kinetics model was appropriate for oxidative torrefaction because the oxygen further reacts with the solids. These gas–solid reactions are included to account for the effect of oxygen on the decomposition procedure.

MATLAB is a programming platform suitable for systems/product analysis/predictions/design by scientists/engineers. It uses a matrix-based programming language, letting natural expression of computational mathematics. It can be used on laboratory and industrial scales. It can be used for a numerical methodology to fit torrefaction kinetic parameters by minimizing the sum of squares function of experimental/model results. Nonlinear torrefaction optimization can be achieved by using the MATLAB command 'lsqcurvefit' with the default tolerance settings, which is based on the Niedler–Mead optimization algorithm for the minimization of the mean square between calculated/experimental data. The torrefaction kinetic parameters can be estimated by a non-negative linear least-squares method via the 'lsqnonneg' algorithm in MATLAB or by an implemented nonlinear least-squared method, fitting simultaneously the experimental results for all temperature/oxygen concentration sets.

The knowledge of the chemistry of the torrefaction reactions and the thermodynamic analysis of this process is crucial in evaluating the technology feasibility, using a system analysis software called Cycle-Tempo, version 5.1. (Process & Energy Department of the Delft University of Technology, Delft, Holland) a steady state simulation model of this process combining drying and torrefaction unit operation blocks with supplementary process apparatus [205]. The process simulation for numerous inputs can forecast the system efficiency in correlation with the torrefaction temperatures and feedstock moisture percentage. The Cycle-Tempo software can be applied for the process flow designing within a reasonable heat integration strategy approach and feasible sizing of process equipment.

Cycle-Tempo is a flow sheeting tool for the thermodynamic analysis and optimization of energy conversion systems. It is suitable for modeling the off-design behavior of turbines, heat exchangers, flash heaters, condensers, and pipes. It is appropriate for conventional and unconventional power plants/energy systems, and it is capable of exergy analysis. It is suitable for the development of wood waste pretreatment equilibrium models based on the Gibbs free energy minimization approach via non-complex and complex models.

Liu et al. [38] established a new lumped model to investigate the reaction mechanism of rice straw and husk decomposition by torrefaction. This model was validated by fitting the experimental data. The simulation gave the van Krevelen diagram, i.e., C/O and C/H ratio diagram, and the CHO index, i.e., the carbon's oxidation state in organic pyrolysis products. The 'loss of O/loss of energy' parameter was defined to be related to the energy efficiency of this process. The optimum torrefaction temperature for rice husks and straw was determined using the Chemkin model. The simulation provided data on the whole temperature range, indicating the experimental defects such as high cost and time. The van Krevelen diagram in combination with 'loss of O/loss of energy' and CHO

index and the new parameter offered valuable evidence on feedstock torrefaction and the relationship among the various indexes, offering some significant perceptions and direction for torrefaction simulation and optimization.

A two-dimensional, single-particle, transient model was created by Okekunle [140] for lignocellulosic feedstock torrefaction. A porous solid simulated a wood cylinder, while the finite volume method was applied to simulate the evolution equations for energy conservation, transport, and intra-particle pressure. The tridiagonal matrix algorithm was used to solve the formed linear algebraic equations. Darcy's law gave the intra-particle flow velocity. Intra-particle temperature profile and mass loss record simulation results fitted satisfactorily with the literature data. As regards the interior of the particle, thermal flux, torrefaction fronts, and drying developed in a semi-ellipsoidal structure. Volatile releases were mostly water vapor. The loss of water and carbon dioxide resulted in a decrease in mass and energy yield. The two-dimensional, single particle, transient model can be applied in a broad variety of conditions as valuable software in lignocellulosic feedstock torrefaction pretreatment. In addition, the evidence from weight loss curves, SEM images, HHV, and numerical simulation can be used to forecast the difference in bulk arrangements contributed to different decomposition pathways [206]. The hollow bulk arrangement can contribute to a decomposition pathway which can be described by using the two-step reaction in the series model. The compact bulk arrangement can result in an autocatalytic decomposition pathway and a higher level of decomposition. This increasing level consequently can lead to an HHV enhancement contrasted to the empty mass arrangement.

TGA can be used to examine the kinetics and thermal degradation during the torrefaction of lignocellulosic feedstock [24]. Bach and Chen [30], expressed the torrefaction kinetics using the Arrhenius law including activation energy, frequency factor, and reaction order. TGA is considered a valuable classification technique in defining the degradation kinetics and thermal performance of lignocellulosic feedstock [32,48,161].

Gajera et al. [36] examined the wheat straw physicochemical performance and the groundnut stalk behavior to be used as feedstock for the torrefaction process. TGA was used to monitor the torrefaction process at various isothermal heating rates. Results showed significant hemicellulose and volatile percentage decrease improving HHV, i.e., improving the fuel properties by elevating torrefaction temperature, decreasing volatile content, and increasing carbon content and heating value. The activation energy was found by kinetic parameter analysis with (i) Ozawa–Flynn–Wall and (ii) Starink models. These results offer significant fundamental data assistance for the thermochemical conversion of biomass feedstock.

According to Sasongko et al. [207], a few models focus on the hardwood biomass torrefaction process. Consequently, they developed a simple model to estimate the optimal mass and energy yield. A combination of kinetic, and mass/energy balance models was established. The kinetic model involved: (i) chemical kinetics and (ii) heat transfer. The three parallel reactions (TPR) simulation predicted the degradation of feedstock using three parallel and independent reactions of char, tar, and gas. The two-stage reaction model (TSR) was based on the single hemicellulose decomposition approach. The Elemental Reaction (ER) model separated the degradation reaction from the various components of biomass, i.e., hemicelluloses, cellulose, and lignin, because biomass is primarily a lignocellulosic feedstock.

Kinetic and thermochemical models were established for poplar wood torrefaction to satisfactorily fit the experimental torrefaction TGA data. They offered a consistent picture of the progress of the produced solid and volatile products as well as chemical elements percentage. These models illustrated the poplar wood torrefaction thermochemical performing. They displayed that (i) high temperature increases the product's evolution rate favoring volatiles' formation while the heating rate has a slight effect on this; (ii) temperature and time significantly affect energy and mass yields; and (iii) torrefaction is primarily endother-

mic. This simulation approach offers theoretical assistance for potential valorization and optimization of woody feedstock torrefaction facilities [208].

5.1.3. Torrefaction Severity Factor- and Torrefaction Severity Index-Based Models

Torrefaction severity factor (TSF)- [6,139,209,210] and torrefaction severity index (TSI)- [211] based models are very useful as regards biomass torrefaction simulation. Yu et al. [6] correlated the properties of several samples of torrefied lignocellulosic feedstock to improve the design of the process and predict the torrefaction severity on a commercial scale. These properties were functions of mass yield as regards wood kenaf, pellets/chips, and rice straw/husk commercial samples. Good fitting was achieved for volatile matter/fixed carbon ratio, elemental composition, and HHV vs. mass yield. The applied methodology calculated the torrefaction severity based on the reaction characteristics measured by the TGA technique. Furthermore, during torrefaction the amount of fixed carbon increased compared to the raw biomass, suggesting polymerization reactions and cross-linking. The torrefied biomass energy density was a function of the raw biomass compaction degree and the process severity. The torrefied feedstock grindability of was like that of coal from woody samples and kenaf.

Zhang et al. [211] correlated severity, torrefaction performance, and energy usage for biochar production. Spent coffee grounds, Chinese medicine residue, and microalga residue were torrefied in a nitrogen environment for biochar production. Enhancement factors of HHV, decarbonization, dehydrogenation, deoxygenation, energy yield, and atomic O/C and H/C ratios were studied. The dimensionless parameter TSI, i.e., the weight loss of feedstock, was sufficiently correlated with biochar properties. The O/C ratio was the exception. The upgrading energy index (UEI) was related to the energy reaction efficiency. UEI decreased with TSI increasing, meaning that biochar quality and HHV were optimized at a high TSI.

Thermal energy content enhancement of barley straw via torrefaction was correlated with the process parameters, i.e., time and temperature, and kinetic models were developed to fit the experimental data. TSF was used, combining the process temperature and time effect into a single reaction ordinate [163]. Maximum HHV was achieved at the most severe torrefaction conditions. Torrefied barley straw was found to be a potential alternative renewable energy source, i.e., a coal substitute or an activated carbon low-cost substitute within the biorefinery and the circular economy concept. Gonzalez-Arias et al. [173] used the TSF to compare different processes, (i) hydrothermal carbonization, (ii) pyrolysis, and (iii) torrefaction of olive tree pruning. This parameter is related to the reaction temperature and time of every run. This allowed understanding of the effect of the reaction parameters on the char produced.

5.1.4. Commercial Simulation Software

Manouchehrinejad and Mani [212], developed a thermodynamic-based process simulation model for an integrated torrefaction–pelletization facility. They used Aspen Plus simulation tool for mass/energy balances, design parameters, and equipment size estimation. Feedstock drying, fuel combustion, torrefaction, grinding, pelletizing, and cooling were the basic unit operations. Moreover, they simulated temperature profiles and moisture content of solids and hot gas for a solid convective rotary dryer. In addition, they simulated the main thermal and electrical energy requirements of a rotary kiln torrefaction reactor using the pre-defined reactor modules methodology. HHV, mass/energy yield, and torgas compositions were the output parameters of the torrefaction reactor. Combustion, grinding, pelletization, and cooling were the major unit operations simulated to perform thermodynamic mass/energy balances at industrial scale pine wood chip feedstock. A separate solid fuel burner unit was simulated in the case that wood bark auxiliary fuel was replacing natural gas. Torrefied pellets production total thermal energy consumption to was estimated. The established simulation can be used to perform commercial-scale process economics/safety assessments. Awang et al. [213] developed an Aspen Plus simulation

approach for pelletization via torrefied using empty fruit bunch. Maximum mass yield and minimum energy requirement were the optimization criteria. The produced pellets had enhanced HHV, brittle, high bulk energy density, and increased hydrophobicity like coal and low cost of power demand.

Aspen Plus commercial process simulation software Version 14 (by AspenTech Inc., Bedford, MA, USA) is the most popular modeling tool as regards laboratory and industrial scale facilities. It is usually applied for simulating biomass gasification while the usage of a pre-defined reactor in this to simulate torrefaction is more difficult due to the complexity of this process. This software has been utilized to simulate different lignocellulosic feedstocks' pretreatments under a broad range of operating conditions. The operation unit of torrefaction is displayed in the flow-diagram by operation blocks, indicating material/energy streams. It involves a substantial chemical components property database useful for the calculations, incorporating the required custom-built Fortran or Excel subroutines. It is used to analyze the mass/energy balance in chemical engineering processes by developing equilibrium models appropriate for the highest yield or thermal efficiency forecasting. Its library has many unit operations models for reactions, heat exchange, and separation as well as for the properties of various chemicals. On the other hand, the properties of cellulose, hemicelluloses, and lignin have been defined by National Renewable Energy Lab (NREL), Golden, CO, USA. In conclusion, Aspen Plus can simulate thermochemical conversion processes, involving (i) feedstock decomposition, (ii) volatile reactions, (iii) char combustion, and (iv) condensable/non-condensable gas and gas/solid separation.

Yek et al. [49] simulated the microwave distribution and the microwave heating performance in the cavity using integrated radio frequency and transient heat transfer modules. The COMSOL Multiphysics finite element analysis software (Comsol, Burlington, MA, USA) was applied to predict the temperature profile and microwave electric field of empty fruit bunch pellets. The simulation results satisfactorily fitted the experimental data. The distinctiveness of microwave heating was proved by the enhanced temperature distribution at the center and bottom section of the empty fruit bunch pellet reactor bed. The experimental temperature profile was simulated according to the specific cavity geometry and dielectric properties-based temperature pattern.

COMSOL Multiphysics software is a commercial computer aid engineering software based on finite element analysis, with a significant set of analyzing/solving functions. This software includes modules suitable for electromagnetics, heat transfer, fluid flow, chemical processes, structural mechanics, and acoustics simulation in one environment/workflow. Application Builder is used to develop all types of simulation applications. COMSOL Multiphysics includes numerous pre- and post-processing functions, for both complex scientific problems and large-scale engineering problems simulation, solving simultaneously coupled multiphysics phenomena. It originates from the PDE Toolbox of MATLAB.

5.1.5. Other Simulation Approaches

In the case of torrefaction, lignocellulosic feedstock is degraded leading to anhydrous weight loss (AWL). The assessment model for AWL is appropriate to examine the thermal decomposition of green waste. AWL prediction can be achieved using a two-step reaction in a series model [214].

Quantification of the torrefaction pretreatment impact on the product gas quality result from steam and steam-oxygen mixtures gasification of non-woody lignocellulosic feedstock in high-temperature entrained flow reactors, can be achieved via a gasification chemical equilibrium model. This model predicted the composition of the produced gas as a function of temperature, equivalence ratio, steam-to-solid ratio, and elemental composition of the lignocellulosic feedstock [215].

Dynamic simulation modeling approach [216] can be utilized to evaluate the integration of wood pellet production via torrefaction as well as a supply chain for product distribution. Discrete event and discrete rate simulation approaches were incorporated into the developed model allowing uncertainties, interdependencies, and supply chain

resource constraints (which are generally simplified or ignored in static and deterministic approaches) to be considered. It includes the supply chain from raw materials sources to final product distribution. This simulation approach utilized a wood pellet supply chain, in British Columbia, Canada, assessing the pellets' cost to various markets, energy demand, and CO_2 emissions alongside the supply chain compared with commercial pellets. Torrefaction process integration led to increased energy density and reduced distribution costs giving the chance for obtaining new potential markets.

The gain and loss method was applied to find the optimal conditions for biomass torrefaction, i.e., by comparison of the energy content gain to the final product's biomass weight loss [217]. Torrefaction experiments were simulated by first- to third-order polynomial regression models determining the correlation between calorific value or weight loss and TSF. The optimized TSF was established by the connection of two regression models for weight loss and HHV. The optimal torrefaction conditions were determined.

The kinetics of torrefaction can be used for the examination of the reaction mechanisms, and the simulation and optimization of the processes. The usual empirical reaction model has some theoretical disadvantages in explaining the torrefaction kinetics of lignocellulosic feedstocks. TGA can be used to investigate the beech wood isothermal torrefaction kinetics. The experimental data can be simulated by an nth-order kinetic model. The kinetic parameters of the nth-order model can be optimized using the pattern search method. The fitting to the experimental data showed that the nth-order model satisfactorily predicted these data [218].

Taguchi experimental design (TED) and analysis of variance (ANOVA) [48], can be used to simulate the effects of microwave power, catalyst concentration, and time on energy yield for microalgal biochar from *Chlorella vulgaris* FSP-E residue, which was torrefied with magnesium oxide as a microwave absorber to enhance heating. The TED and ANOVA approaches verified the substantial effects of microwave power and catalyst concentration.

The "model-free" isoconversional approach [219] can be extended in setting up a complete kinetic model, while conventionally, is limited to the activation energy estimation. It is an innovative approach to investigate the thermal degradation kinetic of biomasses when submitted to torrefaction, having a relevant impact in exploiting the potentialities of biomasses in many energies uses.

Other software useful for torrefaction simulation are as follows: (i) ExtendSim (ExtendSim, San Jose, CA, USA) is a simulation software for discrete event, continuous, discrete rate and agent-based and mixed-mode processes simulation; (ii) PolyAnalyst (Megaputer Intelligence Inc., Bloomington, IN, USA) is a system for extracting actionable knowledge hidden in piles of free text and structured data; (iii) Weka (WEKA company, Campbell, CA, USA) is a collection of machine learning algorithms for data mining tasks, containing tools for data preparation, classification, regression, clustering, association rules mining, and visualization; (iv) RStudio (Posit, Boston, MA, USA) is a free and open-source integrated development environment for R, a programming language for statistical computing and graphics; (v) Quantum XL (SigmaZone, Orlando, FL, USA) is statistical software including DoE, General Statistics, and Monte Carlo Simulation; (vi) Design-Expert (Stat-Ease Inc., Minneapolis, MN, USA) is a statistical software package specialized to develop DoE; and (vii) OriginLab (OriginLab, Northampton, MA, USA) is a DoE application for determining the correlation between process factors and process output useful to design/analyze/optimize an experimental setup.

The simulations of the lignocellulosic biomass dry torrefaction process approaches are presented in Table 7. Moreover, the same simulation approaches are displayed schematically in Figure 3.

Table 7. Simulation of lignocellulosic biomass dry torrefaction process.

Simulation	Material	Forecasting	Model	Software	Reference
AWL approach	Green waste	TGA	Di Blasi and Lanzetta	MATLAB	[214]
Chemical equilibrium	Tomato peels	Gas composition	Chemical equilibrium		[215]
Commercial	Biomass	Mass, energy, size, cost, safety	Thermodynamic	Aspen Plus	[212]
Commercial	Empty fruit bunch pellet	Temperature profile, microwave electric field		COMSOL Multiphysics	[49]
Commercial	Empty fruit bunch	Mass yield, energy	RKS, RKS-BM, MILP	Aspen Plus	[213]
CTSF	Eucalyptus	TGA			[210]
Dynamic simulation modeling approach	Sawdust, shavings	Cost, energy input, CO_2 emission	PSC	ExtendSim	[216]
Empirical	Corncob, rice husk	HHV, energy yield/density			[194]
Gain and loss method	Eucalyptus, larch, yellow poplar, acacia, albasia, mixed softwood, mesocarp/oil palm residues	Calorific value, weight loss	2^2 factorial experimental design, regression, severity factor	-	[217]
Kinetic approach	Biomass	HHV, mass loss	Kinetics	Cycle-Tempo	[205]
Kinetic approach	Rice husk, rice straw	HHV, energy	Lumped model		[38]
Kinetic approach	Biomass	Intra-particle temperature profile, mass/energy yield	Two-dimensional, transient, single particle		[140]
Kinetic approach	Sugarcane trash	HHV	Two-step reaction in series		[206]
Kinetic approach	Biomass	TGA			[24]
Kinetic approach	Spruce, birch	Biochar yield, elemental composition	Consecutive reactions		[30]
Kinetic/ thermochemical approach	Wheat straw, Groundnut stalk	TGA	WFO, Starink method, model-free methods, multiple linear regressions		[36]
Kinetics/ thermochemical approach	Hardwood	Mass/energy yield	TPR, TSR, ER		[206]
Kinetics/ thermochemical approach	Poplar wood	TGA	Kinetic, thermochemical	MATLAB	[208]
MARS, ANN	Microalgae, macroalga, biomass wastes	TSI		Megaputer PolyAnalyst	[197]
MARS-SA	Biomass	HHV			[198]

Table 7. *Cont.*

Simulation	Material	Forecasting	Model	Software	Reference
MLP-ANN	Biomass	HHV		Weka	[198]
Model-free isoconversional approach	Biomass	Arrhenius pre-exponential factor, reaction model function	Coats and Redfern, Malek, Freeman and Carroll, compensation methods		[219]
Multi-objective, ANN	Coffee grounds	TG-FTIR	Kinetic, thermodynamic		[4]
One-dimensional simulation analysis	Wood pellet	HHV		MATLAB	[220]
Pattern search method	Beech wood	TGA	Kinetic	MATLAB	[218]
Proximate/ultimate analyses	Biomass	HHV	Linear, quadratic	MS Excel	[221]
PSO-SVM	Biomass	HHV			[199]
RF	Biomass	HHV		Weka	[199]
RF-SA	Biomass	HHV			[198]
Severity factor	Barley straw	HHV, energy yield, enhancement factor	Kinetics		[163]
Severity factor	Olive tree pruning	Product yield, solid quality, energy consumption, HHV		-	[173]
Statistical analysis	Sugarcane leaves	Energy/mass yield, proximate/ultimate analyses, fiber analysis, HHV, FTIR structural parameters, O/C ratio, H/C ratio		R Studio	[41]
SVM-SA	Biomass	HHV			[198]
Taguchi approach	*Chlorella vulgaris* FSP-E	Energy yield, HHV, TGA, UEI	TED, ANOVA		[48]
Thermodynamic	Biomass	Torrefier design	Heat and mass transfer	MS Excel	[139]
TSF	Wood chips, wood pellets, kenaf, rice straw, rice husk	TGA, HHV, VM, TTBGI	Correlations		[6]
TSF	Spent coffee grounds *Arthrospira platensis* residue, C. sp. JSC4, Chinese medicine residue	HHV, energy densification/yield	Linear		[209]
TSI	Spent coffee grounds, Chinese medicine residue, microalga residue	HHV enhancement factor, energy yield, decarbonization, dehydrogenation, deoxygenation, O/C, H/C	Correlations		[211]

Table 7. *Cont.*

Simulation	Material	Forecasting	Model	Software	Reference
TSR	Chinese fir, corn stalk, palm kernel shell	Ultimate/proximate analysis, mass/energy yields	Quadratic equation		[222]
TSR-PSO	Lignocellulosic biomass	TG-FTIR	Isothermal kinetics		[32]

ANN = artificial neural network, ANOVA = Analysis of variance, AWL = anhydrous weight loss, CTSF = Catalytic TSF, ER = Elemental Reaction, HHV = higher heating value, MARS = multivariate adaptive regression splines, MILP = mixed integer linear programming, MLP = multilayer perceptron neural network, PSC = Pellet Supply Chain, PSO = particle swarm optimization, RF = Random Forest, RKS = Readlich–Kwong–Soave cubic equation of state, RKS-BM = Boston–Mathias alpha function, SA = Simulated annealing, SVM = Support vector machine, TED = Taguchi experimental design, TGA = Thermogravimetric analysis, TPR = Three Parallel Reaction mechanism, TSF = Torrefaction severity factor, TSI = Torrefaction severity index, TSR = two-stage reaction model, TTBGI = thermally treated biomass grindability index, UEI = Upgrading energy index, WFO = Wall–Flynn–Ozawa isoconversional method.

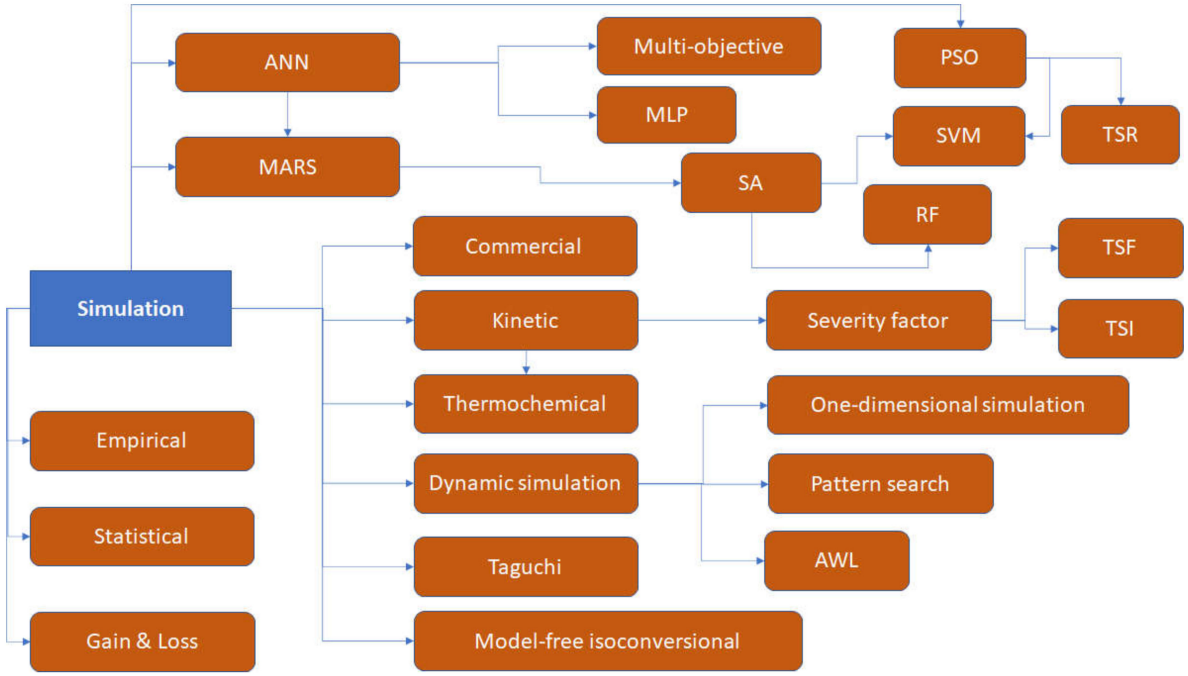

Figure 3. Simulation of dry torrefaction process.

5.2. Simulation of the Lignocellulosic Biomass Wet Torrefaction Process

Chen et al. [223] used AI for forecast and the data were supplied to machine learning. Data analysis was used for torrefaction operating conditions optimization, maximum glucose fermentable to bioethanol concentration while wet torrefaction was used as lignocellulosic feedstock pretreatment. Forty-nine data sets were split for training and testing material. NN and MARS, combined with a decision tree (DT) were applied to forecast five different feedstocks' glucose concentrations and feedstock classification. The NN forecasts had better fitting than the MARS results. The NN approach was used for the glucose prediction in combination with the Box–Behnken design of experiments (DoE). Consequently, NN is an appropriate approach to glucose fermentable to bioethanol forecasting from wet-torrefied biomass. Moreover, the ANOVA approach proved that sulfuric acid catalyst concentration affects more the produced glucose concentration, compared to reaction temperature and time.

Nazos et al. [54], investigated the possibility of improving the barley straw HHV, using acid-catalyzed wet torrefaction (ACWT), well known as acid hydrolysis, in an autoclave (batch reactor). Moreover, (i) combined severity factor (CSF) and (ii) response surface methodology (RSM) based on Box–Behnken DoE were utilized as simulation approaches.

The ACWT parameters were sulfuric acid concentration, temperature, and time. The pretreated product's HHV was significantly affected by the straw composition alterations during ACWT. González-Arias et al. [173], applied CSF for solid biofuel production by hydrothermal carbonization of olive tree pruning.

RSM was used by Gan et al. [169] to simulate and optimize the palm kernel shell wet torrefaction energy-efficient conditions. Among several operating conditions such as temperature, time, and palm kernel shell/water ratio, it was found that temperature showed an extremely substantial impact on the produced fuel properties. TGA verified that wet-torrefied feedstock presented a superior combustion performance. Higher carbon percentage, lower oxygen percentage, and lower ash percentage of the wet-torrefied feedstock enhanced the fuel value.

The simulations of the lignocellulosic biomass wet torrefaction process approaches are presented in Table 8. Moreover, the same simulation approaches are displayed schematically in Figure 4.

Table 8. Simulation of lignocellulosic biomass wet torrefaction process.

Simulation	Material	Forecasting	Design	Model	Software	Reference
ANN, DT	Microalgae (*Chlorella vulgaris* ESP-31, *Chlorella* sp. GD, *Chlorella vulgaris* FSP-E)	Glucose	Box–Behnken	Quadratic		[223]
CSF	Barley straw	HHV, EF, EY, SRY	Box–Behnken	Quadratic	Quantum XL	[54]
CSF	Olive tree pruning	SRY, solid quality, energy consumption, HHV				[173]
Kinetic analysis	Bamboo sawdust/plastic	Activation energy		KAS, OFW, FM		[31]
Kinetic analysis	Spruce/birch wood	Decompositions of hemicellulose/cellulose/lignin		Three parallel reactions		[121]
MARS, DT	Microalgae (*Chlorella vulgaris* ESP-31, *Chlorella* sp. GD, *Chlorella vulgaris* FSP-E)	Glucose	Box–Behnken	Quadratic		[223]
RSM	Barley straw	HHV, EF, EY, SRY	Box–Behnken	Quadratic	Quantum XL	[54]
RSM	Palm kernel shell	HHV, SRY	CCD	Quadratic		[169]
RSM	Sludge/pulp/paper	Energy yield	CCD	PCM	Matlab, DesignExpert OriginLab	[224]
Statistical analysis	Sugarcane leaves	SRY, energy yield, proximate/ultimate analyses, fiber analysis, HHV, FTIR structural parameters, O/C, H/C			RStudio	[41]

ANN = artificial neural network, CCD = central composite design, CSF = combined severity factor, DT = Decision Tree, EF = enhancement factor, EY = energy yield, FM = Friedman model, KAS = Kissingere–Akahirae–Sunose model, MARS = multivariate adaptive regression splines, OFW = Ozawae–Flynne–Wall model, PCM = principal component model, RSM = response surface methodology, SRY = solid residue yield.

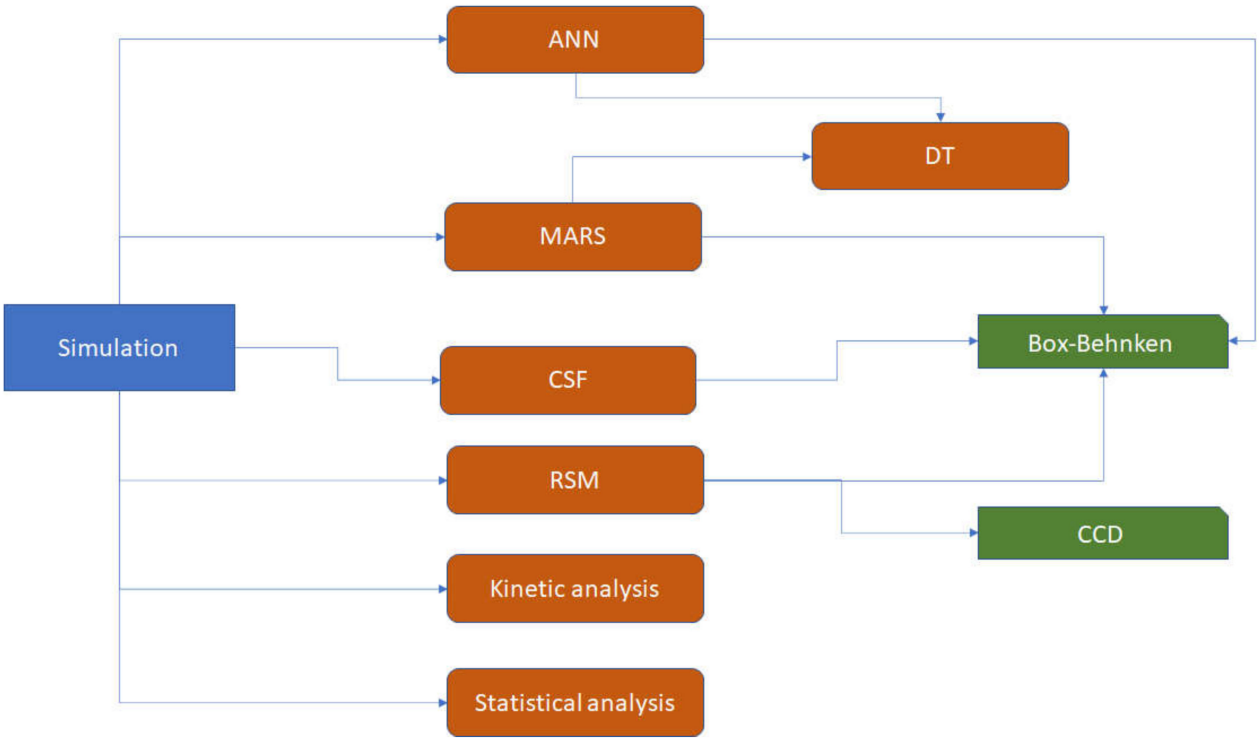

Figure 4. Simulation of wet torrefaction process.

5.3. Optimization of the Lignocellulosic Biomass Wet and Dry Torrefaction Process

ANN is a data-driven model appropriate for the multi-objective optimization of the lignocellulosic feedstock torrefaction process and can robustly and accurately forecast the nonlinear relationships between the multiple inputs and outputs regardless of parametric and nonparametric distributions with missing values [19,49,225,226]. The hyperparameters of the ANN model can be selected and tuned to obtain the best-fit from the performance measures of the root mean squared error and the coefficient of determination of a random 5-fold cross-validation. The joint optimization with the best-fit ANN can be performed based on the criteria of composite desirability [4].

Oh et al. [220] attempted to optimize the torrefaction of woody biomass using one-dimensional simulation analysis. Changes in the elemental contents of biomass were predicted by analyzing the mass reduction and characteristics of volatile matter emission due to torrefaction, and changes in the calorific value were derived. Comparing experiments and simulations estimated the calorific value and optimal conditions according to the process temperature and time, providing preliminary findings for the effective utilization of biomass, a material that is usually discarded.

More or less, all the above-described simulation approaches, i.e., kinetic/thermodynamic/thermochemical models, severity factors, response surface methodology models, artificial neural networks, multilayer perceptron neural networks, multivariate adaptive regression splines, mixed integer linear programming, Taguchi experimental design, particle swarm optimization, model-free isoconversional approach, dynamic simulation modeling, and commercial simulation software, can be used for the torrefaction process optimization.

6. Conclusions

The simulation and optimization of dry- and wet-torrefaction processing of lignocellulosic biomass was investigated. It was found that the most significant dry- and wet-torrefaction processes simulation/optimization approaches are kinetic/thermodynamic/thermochemical models, severity factors/indexes (TSF, TSI, CSF, UEI), artificial neural networks, and commercial simulation software. In addition, response surface methodology, multilayer perceptron neural networks, multivariate adaptive regression splines,

mixed integer linear programming, Taguchi experimental design, particle swarm optimization, model-free isoconversional approach, and dynamic simulation modeling can be applied as regards the dry/wet torrefaction processes simulation/optimization. In conclusion, torrefaction process simulation applications accelerate the optimization of the pretreatment conditions.

Author Contributions: Conceptualization, A.N.; investigation, G.G.; visualization, D.P.; supervision, D.S. All authors have read and agreed to the published version of the manuscript.

Funding: This research received no external funding.

Data Availability Statement: The study does not report any data.

Acknowledgments: The authors would like to acknowledge administrative and technical support from the University of Piraeus Research Center.

Conflicts of Interest: The authors declare no conflict of interest.

References

1. Thengane, S.K.; Kung, K.S.; Gomez-Barea, A.; Ghoniem, A.F. Advances in biomass torrefaction: Parameters, models, reactors, applications, deployment, and market. *Prog. Energy Combust. Sci.* **2022**, *93*, 101040. [CrossRef]
2. Kota, K.B.; Shenbagaraj, S.; Sharma, P.K.; Sharma, A.K.; Ghodke, P.K.; Chen, W.-H. Biomass torrefaction: An overview of process and technology assessment based on global readiness level. *Fuel* **2022**, *324*, 124663. [CrossRef]
3. Piersa, P.; Unyay, H.; Szufa, S.; Lewandowska, W.; Modrzewski, R.; Slezak, R.; Ledakowicz, S. An Extensive Review and Comparison of Modern Biomass Torrefaction Reactors vs. Biomass Pyrolysis—Part 1. *Energies* **2022**, *15*, 2227. [CrossRef]
4. Fu, J.; Liu, J.; Xu, W.; Chen, Z.; Evrendilek, F.; Sun, S. Torrefaction, temperature, and heating rate dependencies of pyrolysis of coffee grounds: Its performances, bio-oils, and emissions. *Bioresour. Technol.* **2022**, *345*, 126346. [CrossRef] [PubMed]
5. Safin, R.R.; Safina, A.V.; Baigildeeva, E.I.; Kainov, P.A.; Saerova, K.V. Impact of wood raw materials movement parameters on the annealing reactor torrefaction efficiency. *Int. Multidiscip. Sci. GeoConference SGEM* **2020**, *20*, 77–82. [CrossRef]
6. Yu, S.; Kim, H.; Park, J.; Lee, Y.; Park, Y.; Ryu, C. Relationship between torrefaction severity, product properties, and pyrolysis characteristics of various biomass. *Int. J. Energy Res.* **2022**, *46*, 8145–8157. [CrossRef]
7. Potnuri, R.; Suriapparao, D.V.; Rao, C.S.; Sridevi, V.; Kumar, A. Effect of dry torrefaction pretreatment of the microwave-assisted catalytic pyrolysis of biomass using the machine learning approach. *Renew. Energy* **2022**, *197*, 798–809. [CrossRef]
8. Yang, T.; Jie, Y.; Li, B.; Kai, X.; Li, R. The Effect of Different Pretreatments on Biomass Liquefaction. In Proceedings of the ICOPE 2015—International Conference on Power Engineering, Yokohama, Japan, 30 November–4 December 2015.
9. Chen, W.-H.; Chen, C.-J.; Hung, C.-I. Taguchi approach for co-gasification optimization of torrefied biomass and coal. *Bioresour. Technol.* **2013**, *144*, 615–622. [CrossRef]
10. Di Giuliano, A.; Gallucci, M.; Malsegna, B.; Lucantonio, S.; Gallucci, K. Pretreated residual biomasses in fluidized beds for chemical looping gasification: Analysis of devolatilization data by statistical tools. *Bioresour. Technol. Rep.* **2022**, *17*, 100926. [CrossRef]
11. Nunes, L.J.R. Biomass gasification as an industrial process with effective proof-of-concept: A comprehensive review on technologies, processes and future developments. *Results Eng.* **2022**, *14*, 100408. [CrossRef]
12. Sarker, T.R.; Nanda, S.; Meda, V.; Dalai, A.K. Process optimization and investigating the effects of torrefaction and pelletization on steam gasification of canola residue. *Fuel* **2022**, *323*, 124239. [CrossRef]
13. Van der Stelt, M.J.C.; Gerhauser, H.; Kiel, J.H.A.; Ptasinski, K.J. Biomass upgrading by torrefaction for the production of biofuels: A review. *Biomass Bioenergy* **2011**, *35*, 3748–3762. [CrossRef]
14. Chew, J.J.; Doshi, V. Recent advances in biomass pretreatment –Torrefaction fundamentals and technology. *Renew. Sustain. Energy Rev.* **2011**, *15*, 4212–4222. [CrossRef]
15. Gan, Y.Y.; Ong, H.C.; Show, P.L.; Ling, T.C.; Chen, W.H.; Yu, K.L. Torrefaction of microalgal biochar as potential coal fuel and application as bio-adsorbent. *Energy Convers. Manag.* **2018**, *165*, 152–162. [CrossRef]
16. Pilon, G.; Lavoie, J.M. Characterization of switchgrass char produced in torrefaction and pyrolysis conditions. *BioResources* **2011**, *6*, 16.
17. Misni, S.S.; Kasmuri, N.H.; Subari, F.; Abdullah, Z.; Hanipah, S.H. Bio-coal optimization study of dry leaves via low-temperature mechanism. *Malays. J. Anal. Sci.* **2021**, *25*, 1056–1067.
18. Sharma, H.B.; Sarmah, A.K.; Dubey, B. Hydrothermal carbonization of renewable waste biomass for solid biofuel production: A discussion on process mechanism, the influence of process parameters, environmental performance and fuel properties of hydrochar. *Renew. Sustain. Energy Rev.* **2020**, *123*, 109761. [CrossRef]
19. Sun, Y.; He, Z.; Tu, R.; Wu, Y.; Jiang, E.; Xu, X. The mechanism of wet/dry torrefaction pretreatment on the pyrolysis performance of tobacco stalk. *Bioresour. Technol.* **2019**, *286*, 121390. [CrossRef]

20. Chen, W.H.; Kuo, P.C. A study on torrefaction of various biomass materials and its impact on lignocellulosic structure simulated by a thermogravimetry. *Energy* **2010**, *35*, 2580–2586. [CrossRef]
21. Chen, W.H.; Lu, K.M.; Tsai, C.M. An experimental analysis on property and structure variations of agricultural wastes undergoing torrefaction. *Applied Energy* **2012**, *100*, 318–325. [CrossRef]
22. Zheng, A.; Zhao, Z.; Chang, S.; Huang, Z.; Wang, X.; He, F.; Li, H. Effect of torrefaction on structure and fast pyrolysis behavior of corncobs. *Bioresour. Technol.* **2013**, *128*, 370–377. [CrossRef]
23. Khazraie Shoulaifar, T.; DeMartini, N.; Willför, S.; Pranovich, A.; Smeds, A.I.; Virtanen, T.A.P.; Maunu, S.L.; Verhoeff, F.; Kiel, J.H.; Hupa, M. Impact of torrefaction on the chemical structure of birch wood. *Energy Fuels* **2014**, *28*, 3863–3872. [CrossRef]
24. Ong, H.C.; Yu, K.L.; Chen, W.-H.; Pillejera, M.K.; Bi, X.; Tran, K.-Q.; Petrissans, A.; Petrissans, M. Variation of lignocellulosic biomass structure from torrefaction: A critical review. *Renew. Sust. Energ. Rev.* **2021**, *152*, 111698. [CrossRef]
25. Wang, P.; Howard, B.H. Impact of thermal pretreatment temperatures on woody biomass chemical composition, physical properties and microstructure. *Energies* **2018**, *11*, 25. [CrossRef]
26. Wu, F.; Zhang, Y.; Liu, W.; Zhu, N.; Chen, J.; Sun, Z. Comparison of torrefied and lyophilized Dendrobii Officinalis Caulis (*Tiepishihu*) by Fourier transform infrared spectroscopy and two-dimensional correlation spectroscopy. *J. Mol. Struct.* **2020**, *1204*, 127554. [CrossRef]
27. Huang, C.; Li, R.; Tang, W.; Zheng, Y.; Meng, X. Improve Enzymatic Hydrolysis of Lignocellulosic Biomass by Modifying Lignin Structure via Sulfite Pretreatment and Using Lignin Blockers. *Fermentation* **2022**, *8*, 558. [CrossRef]
28. Chen, W.H.; Kuo, P.C. Isothermal torrefaction kinetics of hemicellulose, cellulose, lignin and xylan using thermogravimetric analysis. *Energy* **2011**, *36*, 6451–6460. [CrossRef]
29. Bates, R.B.; Ghoniem, A.F. Biomass torrefaction: Modeling of volatile and solid product evolution kinetics. *Bioresour. Technol.* **2012**, *124*, 460–469. [CrossRef]
30. Bach, Q.V.; Chen, W.H.; Chu, Y.S.; Skreiberg, Ø. Predictions of biochar yield and elemental composition during torrefaction of forest residues. *Bioresour. Technol.* **2016**, *215*, 239–246. [CrossRef]
31. Alam, M.; Rammohan, D.; Peela, N.R. Catalytic co-pyrolysis of wet-torrefied bamboo sawdust and plastic over the zeolite H-ZSM-5: Synergistic effects and kinetics. *Renew. Energy* **2021**, *178*, 608–619. [CrossRef]
32. Chen, W.H.; Fong Eng, C.; Lin, Y.Y.; Bach, Q.V.; Ashokkumar, V.; Show, P.L. Two-step thermodegradation kinetics of cellulose, hemicelluloses, and lignin under isothermal torrefaction analyzed by particle swarm optimization. *Energy Convers. Manag.* **2021**, *238*, 114116. [CrossRef]
33. Gan, Y.Y.; Chen, W.H.; Ong, H.C.; Lin, Y.Y.; Sheen, H.K.; Chang, J.S.; Ling, T.C. Effect of wet torrefaction on pyrolysis kinetics and conversion of microalgae carbohydrates, proteins, and lipids. *Energy Convers. Manag.* **2021**, *227*, 113609. [CrossRef]
34. Silveira, E.A.; Macedo, L.; Rousset, P.; Commandré, J.-M.; Galvão, L.G.O.; Chaves, B.S. The effect of potassium carbonate wood impregnation on torrefaction kinetics. In Proceedings of the 29th European Biomass Conference and Exhibition, Online, 26–29 April 2021; pp. 1010–1014.
35. Yen, S.-W.; Chen, W.-H.; Chang, J.-S.; Eng, C.-F.; Naqvi, S.R.; Show, P.L. Torrefaction thermogravimetric analysis and kinetics of sorghum distilled residue for sustainable fuel production. *Sustainability* **2021**, *13*, 4246. [CrossRef]
36. Gajera, B.; Tyagi, U.; Sarma, A.K.; Jha, M.K. Impact of torrefaction on thermal behavior of wheat straw and groundnut stalk biomass: Kinetic and thermodynamic study. *Fuel Commun.* **2022**, *12*, 100073. [CrossRef]
37. Lee, B.-H.; Trinh, V.T.; Kim, S.-M.; Jeon, C.-H. Pyrolysis of kenaf (*Hibiscus cannabinus* L.) biomass: Influence of ashless treatment on kinetics and thermal behavior. *J. Therm. Anal. Calorim.* **2022**, *147*, 7399–7410. [CrossRef]
38. Liu, Q.; Chen, C.; Ji, G.; Li, A. Development and application of a detailed kinetic model to evaluate the torrefaction process of rice-based biomass. *Biomass Conv. Bioref.* **2022**. [CrossRef]
39. González-Arias, J.; Sánchez, M.E.; Cara-Jiménez, J. Profitability analysis of thermochemical processes for biomass-waste valorization: A comparison of dry vs wet treatments. *Sci. Total Environ.* **2022**, *811*, 152240. [CrossRef]
40. Isemin, R.; Mikhalev, A.; Milovanov, O.; Klimov, D.; Kokh-Tatarenko, V.; Brulé, M.; Tabet, F.; Nebyvaev, A.; Kuzmin, S.; Konyakhin, V. Comparison of Characteristics of Poultry Litter Pellets Obtained by the Processes of Dry and Wet Torrefaction. *Energies* **2022**, *15*, 2153. [CrossRef]
41. Khempila, J.; Kongto, P.; Meena, P. Comparative study of solid biofuels derived from sugarcane leaves with two different thermochemical conversion methods: Wet and dry torrefaction. *Bioenergy Res.* **2022**, *15*, 1265–1280. [CrossRef]
42. Diker, İ.; Ozkan, G.M. An investigation on implementing wet torrefaction to dewatered poultry sludge. *Biomass Conv. Bioref.* **2022**. [CrossRef]
43. Kudo, S.; Okada, J.; Ikeda, S.; Yoshida, T.; Asano, S.; Hayashi, J.-I. Improvement of Pelletability of Woody Biomass by Torrefaction under Pressurized Steam. *Energy Fuels* **2019**, *33*, 11253–11262. [CrossRef]
44. Negi, S.; Jaswal, G.; Dass, K.; Mazumder, K.; Elumalai, S.; Roy, J.K. Torrefaction: A sustainable method for transforming of agri-wastes to high energy density solids (biocoal). *Rev. Environ. Sci. Bio/Technol.* **2020**, *19*, 463–488. [CrossRef]
45. Yu, Y.; Wu, J.; Ren, X.; Lau, A.; Rezaei, H.; Takada, M.; Bi, X.; Sokhansanj, S. Steam explosion of lignocellulosic biomass for multiple advanced bioenergy processes: A review. *Renew. Sust. Energ. Rev.* **2022**, *154*, 111871. [CrossRef]
46. Arpia, A.A.; Chen, W.-H.; Lam, S.S.; Rousset, P.; de Luna, M.D.G. Sustainable biofuel and bioenergy production from biomass waste residues using microwave-assisted heating: A comprehensive review. *J. Chem. Eng.* **2021**, *403*, 126233. [CrossRef]

47. Zhang, C.; Ho, S.-H.; Chen, W.-H.; Eng, C.F.; Wang, C.-T. Simultaneous implementation of sludge dewatering and solid biofuel production by microwave torrefaction. *Environ. Res.* **2021**, *195*, 110775. [CrossRef]
48. Chen, W.-H.; Arpia, A.A.; Chang, J.-S.; Kwon, E.E.; Park, Y.-K.; Culaba, A.B. Catalytic microwave torrefaction of microalga *Chlorella vulgaris* FSP-E with magnesium oxide optimized via taguchi approach: A thermo-energetic analysis. *Chemosphere* **2022**, *290*, 133374. [CrossRef]
49. Yek, P.N.Y.; Kong, S.H.; Law, M.C.; Xia, C.; Keey Liew, R.; Sung Sie, T.; Lim, J.W.; Lam, S.S. Microwave Torrefaction of Empty Fruit Bunch Pellet: Simulation and Validation of Electric Field and Temperature Distribution. *J. Bioresour. Bioprod.* **2022**, *7*, 270–277. [CrossRef]
50. Kichatov, B.V.; Korshunov, A.M.; Kiverin, A.D.; Yakovenko, I.S. Oxidative Torrefaction of Wood Biomass in a Layer of Mineral Filler. *Eng. Phys. Thermophys.* **2021**, *94*, 738–744. [CrossRef]
51. Zhao, Z.; Feng, S.; Zhao, Y.; Wang, Z.; Ma, J.; Xu, L.; Yang, J.; Shen, B. Investigation on the fuel quality and hydrophobicity of upgraded rice husk derived from various inert and oxidative torrefaction conditions. *Renew. Energy* **2022**, *189*, 1234–1248. [CrossRef]
52. Kadam, R.; Pawar, A.; Panwar, N.L. Environmental Effects Experimental investigation on non-oxidative biomass torrefaction system. *Energy Sources Part A Recovery Util. Environ. Eff.* **2020**, *2020*, 1–13. [CrossRef]
53. Manatura, K. Inert torrefaction of sugarcane bagasse to improve its fuel properties. *Case Stud. Therm. Eng.* **2020**, *19*, 100623. [CrossRef]
54. Nazos, A.; Grammelis, P.; Sakellis, E.; Sidiras, D. Acid-catalyzed wet torrefaction for enhancing the heating value of barley straw. *Energies* **2020**, *13*, 1693. [CrossRef]
55. Gan, Y.Y.; Ong, H.C.; Chen, W.H.; Sheen, H.K.; Chang, J.S.; Chong, C.T.; Ling, T.C. Microwave-assisted wet torrefaction of microalgae under various acids for coproduction of biochar and sugar. *J. Clean. Prod.* **2020**, *253*, 119944. [CrossRef]
56. Yu, K.L.; Chen, W.-H.; Sheen, H.-K.; Chang, J.-S.; Lin, C.-S.; Ong, H.C.; Show, P.L.; Ling, T.C. Bioethanol production from acid pretreated microalgal hydrolysate using microwave-assisted heating wet torrefaction. *Fuel* **2020**, *279*, 118435. [CrossRef]
57. Yu, K.L.; Chen, W.-H.; Sheen, H.-K.; Chang, J.-S.; Lin, C.-S.; Ong, H.C.; Show, P.L.; Ng, E.-P.; Ling, T.C. Production of microalgal biochar and reducing sugar using wet torrefaction with microwave-assisted heating and acid hydrolysis pretreatment. *Renew. Energy* **2020**, *156*, 349–360. [CrossRef]
58. Ku Ismail, K.S.; Matano, Y.; Sakihama, Y.; Inokuma, K.; Nambu, Y.; Hasunuma, T.; Kondo, A. Pretreatment of extruded Napier grass by hydrothermal process with dilute sulfuric acid and fermentation using a cellulose-hydrolyzing and xylose-assimilating yeast for ethanol production. *Bioresour. Technol.* **2022**, *343*, 126071. [CrossRef]
59. Li, M.-F.; Shen, Y.; Sun, J.-K.; Bian, J.; Chen, C.-Z.; Sun, R.-C. Wet Torrefaction of Bamboo in Hydrochloric Acid Solution by Microwave Heating. *ACS Sustain. Chem. Eng.* **2015**, *3*, 2022–2029. [CrossRef]
60. Lynam, J.G.; Coronella, C.J.; Yan, W.; Reza, M.T.; Vasquez, V.R. Acetic acid and lithium chloride effects on hydrothermal carbonization of lignocellulosic biomass. *Bioresour. Technol.* **2011**, *102*, 6192–6199. [CrossRef]
61. Hu, J.; Jiang, B.; Wang, J.; Qiao, Y.; Zuo, T.; Sun, Y.; Jiang, X. Physicochemical characteristics and pyrolysis performance of corn stalk torrefied in aqueous ammonia by microwave heating. *Bioresour. Technol.* **2019**, *274*, 83–88. [CrossRef]
62. Li, C.; Zhu, L.; Ma, Z.; Yang, Y.; Cai, W.; Ye, J.; Qian, J.; Liu, X.; Zuo, Z. Optimization of the nitrogen and oxygen element distribution in microalgae by ammonia torrefaction pretreatment and subsequent fast pyrolysis process for the production of N-containing chemicals. *Bioresour. Technol.* **2020**, *321*, 124461. [CrossRef]
63. Akbari, M.; Oyedun, A.O.; Gemechu, E.; Kumar, A. Comparative life cycle energy and greenhouse gas footprints of dry and wet torrefaction processes of various biomass feedstocks. *J. Environ. Chem. Eng.* **2021**, *9*, 105415. [CrossRef]
64. Carneiro-Junior, J.A.d.M.; de Oliveira, G.F.; Alves, C.T.; Andrade, H.M.C.; Beisl Vieira de Melo, S.A.; Torres, E.A. Valorization of Prosopis juliflora Woody Biomass in Northeast Brazilian through Dry Torrefaction. *Energies* **2021**, *14*, 3465. [CrossRef]
65. He, Z.; Sun, Y.; Cheng, S.; Jia, Z.; Tu, R.; Wu, Y.; Shen, X.; Zhang, F.; Jiang, E.; Xu, X. The enhanced rich H2 from co-gasification of torrefied biomass and low rank coal: The comparison of dry/wet torrefaction, synergetic effect and prediction. *Fuel* **2021**, *287*, 119473. [CrossRef]
66. Jaideep, R.; Lo, W.H.; Lim, G.P.; Chua, C.X.; Gan, S.; Lee, L.Y.; Thangalazhy-Gopakumar, S. Enhancement of fuel properties of yard waste through dry torrefaction. *Mater. Sci. Energy Technol.* **2021**, *4*, 156–165. [CrossRef]
67. Leng, L.; Yang, L.; Chen, J.; Hu, Y.; Li, H.; Li, H.; Jiang, S.; Peng, H.; Yuan, X.; Huang, H. Valorization of the aqueous phase produced from wet and dry thermochemical processing biomass: A review. *J. Clean. Prod.* **2021**, *294*, 126238. [CrossRef]
68. Ullah, H.; Lun, L.; Riaz, L.; Naseem, F.; Shahab, A.; Rashid, A. Physicochemical characteristics and thermal degradation behavior of dry and wet torrefied orange peel obtained by dry/wet torrefaction. *Biomass Conv. Bioref.* **2021**. [CrossRef]
69. Alam, M.; Rammohan, D.; Bhavanam, A.; Peela, N.R. Wet torrefaction of bamboo saw dust and its co-pyrolysis with plastic. *Fuel* **2021**, *285*, 119188. [CrossRef]
70. He, Q.; Raheem, A.; Ding, L.; Xu, J.; Cheng, C.; Yu, G. Combining wet torrefaction and pyrolysis for woody biochar upgradation and structural modification. *Energy Convers. Manag.* **2021**, *243*, 114383. [CrossRef]
71. Isemin, R.; Marias, F.; Muratova, N.; Kuzmin, S.; Klimov, D.; Mikhalev, A.; Milovanov, O.; Brulé, M.; Tabet, F. Wet Torrefaction of Poultry Litter in a Pilot Unit: A Numerical Assessment of the Process Parameters. *Processes* **2021**, *9*, 1835. [CrossRef]
72. Phuang, Y.W.; Ng, W.Z.; Khaw, S.S.; Yap, Y.Y.; Gan, S.; Lee, L.Y.; Thangalazhy-Gopakumar, S. Wet torrefaction pre-treatment of yard waste to improve the fuel properties. *Mater. Sci. Energy Technol.* **2021**, *4*, 211–223. [CrossRef]

73. Soh, M.; Khaerudini, D.S.; Chew, J.J.; Sunarso, J. Wet torrefaction of empty fruit bunches (EFB) and oil palm trunks (OPT): Effects of process parameters on their physicochemical and structural properties. *South Afr. J. Chem. Eng.* **2021**, *35*, 126–136. [CrossRef]
74. Xue, Y.; Zhou, S.; Leng, E.; Cui, C.; Zhou, Z.; Peng, Y. Comprehensive utilization of agricultural wastes by combined wet torrefaction and pyrolysis. *J. Anal. Appl. Pyrolysis* **2021**, *160*, 105358. [CrossRef]
75. Liu, C.; Duan, X.; Chen, Q.; Chao, C.; Lu, Z.; Lai, Q.; Megharaj, M. Investigations on pyrolysis of microalgae *Diplosphaera* sp. MM1 by TG-FTIR and Py-GC/MS: Products and kinetics. *Bioresour Technol.* **2019**, *294*, 122126. [CrossRef] [PubMed]
76. Bridgeman, T.G.; Jones, J.M.; Shield, I.; Williams, P.T. Torrefaction of reed canary grass, wheat straw and willow to enhance solid fuel qualities and combustion properties. *Fuel* **2008**, *87*, 44–56. [CrossRef]
77. Peng, X.; Ma, X.; Lin, Y.; Guo, Z.; Hu, S.; Ning, X.; Cao, Y.; Zhang, Y. Co-pyrolysis between microalgae and textile dyeing sludge by TG–FTIR: Kinetics and products. *Energy Convers. Manag.* **2015**, *100*, 391–402. [CrossRef]
78. Shuping, Z.; Yulong, W.; Mingde, Y.; Chun, L.; Junmao, T. Pyrolysis characteristics and kinetics of the marine microalgae *Dunaliella tertiolecta* using thermogravimetric analyzer. *Bioresour Technol.* **2010**, *101*, 359–365. [CrossRef]
79. Chen, W.H.; Lu, K.M.; Liu, S.H.; Tsai, C.M.; Lee, W.J.; Lin, T.C. Biomass torrefaction characteristics in inert and oxidative atmospheres at various superficial velocities. *Bioresour. Technol.* **2013**, *146*, 152–160. [CrossRef]
80. Nyakuma, B.B.; Wong, S.L.; Faizal, H.M.; Hambali, H.U.; Oladokun, O.; Abdullah, T.A.T. Carbon dioxide torrefaction of oil palm empty fruit bunches pellets: Characterisation and optimisation by response surface methodology. *Biomass Convers. Biorefinery* **2020**, *12*, 5881–5900. [CrossRef]
81. Thanapal, S.S.; Chen, W.; Annamalai, K.; Carlin, N.; Ansley, R.J.; Ranjan, D. Carbon Dioxide Torrefaction of Woody Biomass. *Energy Fuels* **2014**, *28*, 28,1147–57. [CrossRef]
82. Wang, C.; Peng, J.; Li, H.; Bi, X.T.; Legros, R.; Lim, C.J.; Sokhansanj, S. Oxidative torrefaction of biomass residues and densification of torrefied sawdust to pellets. *Bioresour Technol.* **2013**, *127*, 318–325. [CrossRef]
83. Mei, Y.; Liu, R.; Yang, Q.; Yang, H.; Shao, J.; Draper, C.; Zhang, S.; Chen, H. Torrefaction of cedar- wood in a pilot scale rotary kiln and the influence of industrial flue gas. *Bioresour. Technol.* **2015**, *177*, 355–360. [CrossRef] [PubMed]
84. Uemura, Y.; Omar, W.; Othman, N.A.; Yusup, S.; Tsutsui, T. Torrefaction of Oil Palm EFB in the Presence of Oxygen. *Fuel* **2013**, *103*, 156–160. [CrossRef]
85. Yang, W.; Wu, S.; Wang, H.; Ma, P.; Shimanouchi, T.; Kimura, Y.; Zhou, J. Effect of wet and dry torrefaction process on fuel properties of solid fuels derived from bamboo and Japanese cedar. *BioResources* **2017**, *12*, 8629–8640. [CrossRef]
86. Romanowska-Duda, Z.; Szufa, S.; Grzesik, M.; Piotrowski, K.; Janas, R. The Promotive Effect of *Cyanobacteria* and *Chlorella* sp. Foliar Biofertilization on Growth and Metabolic Activities of Willow (*Salix viminalis* L.) Plants as Feedstock Production, Solid Biofuel and Biochar as C Carrier for Fertilizers via Torrefaction Process. *Energies* **2021**, *14*, 5262.
87. Kuo, P.C.; Wu, W.; Chen, W.H. Gasification performances of raw and torrefied biomass in a downdraft fixed bed gasifier using thermodynamic analysis. *Fuel* **2014**, *117*, 1231–1241. [CrossRef]
88. Basu, P.; Dhungana, A.; Rao, S.; Acharya, B. Effect of oxygen presence in torrefied. *J. Energy Inst.* **2013**, *86*, 171–176. [CrossRef]
89. Acharya, B.; Dutta, A.; Minaret, J. Review on comparative study of dry and wet torrefaction. *Sustain. Energy Technol. Asses.* **2015**, *12*, 26–37. [CrossRef]
90. Yan, W.; Hastings, J.T.; Acharjee, T.C.; Coronella, C.J.; Vásquez, V.R. Mass and energy balances of wet torrefaction of lignocellulosic biomass. *Energy Fuels* **2010**, *24*, 4738–4742. [CrossRef]
91. Kobayashi, N.; Okada, N.; Hirakawa, A.; Sato, T.; Kobayashi, J.; Hatano, S.; Mori, S. Characteristics of solid residues obtained from hot-compressed-water treatment of woody biomass. *Ind. Eng. Chem. Res.* **2008**, *48*, 373–379. [CrossRef]
92. Weil, J.R.; Sarikaya, A.; Rau, S.L.; Goetz, J.; Ladisch, C.M.; Brewer, M.; Hendrickson, R.; Ladisch, M.R. Pretreatment of corn fiber by pressure cooking in water. *Appl. Biochem. Biotechnol.* **1998**, *73*, 1–17. [CrossRef]
93. Funke, A.; Ziegler, F. Hydrothermal carbonization of biomass: A summary and discussion of chemical mechanisms for process engineering. Biofuels. *Bioprod. Biorefin.* **2010**, *4*, 160–177. [CrossRef]
94. Xiao, L.P.; Shi, Z.J.; Xu, F.; Sun, R.C. Hydrothermal carbonization of lignocellulosic biomass. *Bioresour. Technol.* **2012**, *118*, 619–623. [CrossRef] [PubMed]
95. Mumme, J.; Eckervogt, L.; Pielert, J.; Diakite, M.; Rupp, F.; Kern, J. Hydrothermal carbonization of anaerobically digested maize silage. *Bioresour. Technol.* **2011**, *102*, 9255–9560. [CrossRef]
96. Lucian, M.; Fiori, L. Hydrothermal carbonization of waste biomass: Process design, modeling, energy efficiency and cost analysis. *Energies* **2017**, *10*, 211. [CrossRef]
97. Gallifuoco, A.; Papa, A.A.; Spera, A.; Taglieri, L.; Carlo, A.D. Dynamics of liquid-phase platform chemicals during the hydrothermal carbonization of lignocellulosic biomass. *Bioresour. Technol. Rep.* **2022**, *19*, 101177. [CrossRef]
98. Libra, J.A.; Ro, K.S.; Kammann, C.; Funke, A.; Berge, N.D.; Neubauer, Y.; Titirici, M.M.; Fühner, C.; Bens, O.; Kern, J.; et al. Hydrothermal carbonization of biomass residuals: A comparative review of the chemistry, processes and applications of wet and dry pyrolysis. *Biofuels* **2011**, *2*, 89–124. [CrossRef]
99. Hoekman, S.K.; Broch, A.; Robbins, C. Hydrothermal carbonization (HTC) of lignocellulosic biomass. *Energy Fuels* **2011**, *25*, 1802–1810. [CrossRef]
100. Tripathi, A.D.; Mishra, P.K.; Darani, K.K.; Agarwal, A.; Paul, V. Hydrothermal treatment of lignocellulose waste for the production of polyhydroxyalkanoates copolymer with potential application in food packaging. *Trends Food Sci. Technol.* **2022**, *123*, 233–250. [CrossRef]

101. Steinbrecher, T.; Bonk, F.; Scherzinger, M.; Lüdtke, O.; Kaltschmitt, M. Fractionation of Lignocellulosic Fibrous Straw Digestate by Combined Hydrothermal and Enzymatic Treatment. *Energies* **2022**, *15*, 6111. [CrossRef]
102. Jung, J.Y.; Park, H.-M.; Yang, J.-K. Optimization of ethanol extraction of antioxidative phenolic compounds from torrefied oak wood (*Quercus serrata*) using response surface methodology. *Wood Sci. Technol.* **2016**, *50*, 1037–1055. [CrossRef]
103. Amidon, T.E.; Wood, C.D.; Shupe, A.M.; Wang, Y.; Graves, M.; Liu, S. Biorefinery conversion of woody biomass to chemicals, energy and materials. *J. Biobased Mater. Bioenergy* **2008**, *2*, 100–120. [CrossRef]
104. Hsu, W.E.; Schwalds, W.; Schwald, J.; Shields, J.A. Chemical and physical changes required for producing dimensionally stable wood-based composites, Part 1: Steam pretreatment. *Wood Sci. Technol.* **1988**, *22*, 281–289. [CrossRef]
105. Schwald, W.; Brownell, H.H.; Saddler, J.N. Enzymatic hydrolysis of steam treated aspen wood: Influence of partial hemicellulose and lignin removal prior to pretreatment. *J. Wood Chem. Technol.* **2011**, *8*, 543–560. [CrossRef]
106. Agbor, V.; Cicek, N.; Sparling, R.; Berlin, A.; Levin, D. Biomass pretreatment: Fundamentals toward application. *Biotechnol. Adv.* **2011**, *29*, 675–685. [CrossRef]
107. Hill, C. *Wood Modification: Chemical, Thermal and Other Processes*; Wiley: Chichester, UK, 2006.
108. Bobleter, D.; Bonn, G.; Prutsch, W. Steam explosion-hydro thermolysis organosolv a comparison. In *Steam Explosion Techniques: Fundamentals and Industrial Applications*; Focher, B., Marzetti, A., Crescenzi, V., Eds.; Gordon and Breach Science Publishers: Amsterdam, The Netherlands, 1991; pp. 59–82.
109. Bobleter, O.; Bonn, G. The hydrothermolysis of cellobiose and its reaction-product D-glucose. *Carbohydr. Res.* **1983**, *1241*, 85–193. [CrossRef]
110. Harris, E.E. Wood hydrolysis. In *Wood Chemistry*, 2nd ed.; Wise, L.E., Jahn, E.C., Eds.; Reinhold Publishing Corporation: New York, NY, USA, 1952.
111. Wang, L.; Riva, L.; Skreiberg, Ø.; Khalil, R.; Bartocci, P.; Yang, Q.; Yang, H.; Wang, X.; Chen, D.; Rudolfsson, M.; et al. Effect of Torrefaction on Properties of Pellets Produced from Woody Biomass. *Energy Fuels* **2020**, *34*, 15343–15354. [CrossRef]
112. Suchsland, O.; Woodson, G.E.; McMillin, C.W. Effect of cooking conditions on fiber bonding in dry formed binder less hardboard. *For. Prod. J.* **1987**, *37*, 66–69.
113. Chen, W.H.; Ye, S.C.; Sheen, H.K. Hydrothermal carbonization of sugarcane bagasse via wet torrefaction in association with microwave heating. *Bioresour. Technol.* **2012**, *118*, 195–203. [CrossRef] [PubMed]
114. Wu, K.T.; Tsai, C.J.; Chen, C.S.; Chen, H.W. The characteristics of torrefied microalgae. *Appl. Energy* **2012**, *100*, 52–57. [CrossRef]
115. Chen, W.H.; Tu, Y.J.; Sheen, H.K. Impact of dilute acid pretreatment on the structure of bagasse for bioethanol production. *Int. J. Energy Res.* **2010**, *34*, 265–274. [CrossRef]
116. Chen, W.H.; Tu, Y.J.; Sheen, H.K. Disruption of sugarcane bagasse lignocellulosic structure by means of dilute sulfuric acid pretreatment with microwave-assisted heating. *Appl. Energy* **2011**, *88*, 2726–2734. [CrossRef]
117. Zheng, Y.; Yu, Y.; Lin, W.; Jin, ϒ.; Yong, Q.; Huang, C. Enhancing the enzymatic digestibility of bamboo residues by biphasic phenoxyethanol-acid pretreatment. *Bioresour. Technol.* **2021**, *325*, 124691. [CrossRef]
118. Lin, W.; Xing, S.; Jin, Y.; Lu, X.; Huang, C.; Yong, Q. Insight into understanding the performance of deep eutectic solvent pretreatment on improving enzymatic digestibility of bamboo residues. *Bioresour. Technol.* **2020**, *306*, 123163. [CrossRef] [PubMed]
119. Shi, N.; Liu, Q.; Cen, H.; Ju, R.; He, X.; Ma, L. Formation of humins during degradation of carbohydrates and furfural derivatives in various solvents. *Biomass Convers. Biorefinery* **2020**, *10*, 277–287. [CrossRef]
120. Yan, W.; Acharjee, T.C.; Coronella, C.J.; Vásquez, V.R. Thermal pretreatment of lignocellulosic biomass. *Environ. Prog. Sustain.* **2009**, *28*, 435–440. [CrossRef]
121. Bach, Q.V.; Tran, K.Q.; Skreiberg, Ø.; Trinh, T.T. Effects of wet torrefaction on pyrolysis of woody biomass fuels. *Energy* **2015**, *88*, 443–456. [CrossRef]
122. Bach, Q.V.; Chen, W.H.; Lin, S.C.; Sheen, H.K.; Chang, J.S. Wet torrefaction of microalga *Chlorella vulgaris* ESP-31 with microwave-assisted heating. *Energy Convers. Manag.* **2017**, *141*, 163–170. [CrossRef]
123. Balat, M.; Balat, H.; Öz, C. Progress in bioethanol processing. *PECS* **2008**, *34*, 551–573. [CrossRef]
124. Chen, Z.; Wang, M.; Ren, Y.; Jiang, E.; Jiang, Y.; Li, W. Biomass torrefaction: A promising pretreatment technology for biomass utilization. *IOP Conf. Ser. Earth Environ. Sci.* **2018**, *113*, 012201. [CrossRef]
125. Lam, P.S.; Sokhansanj, S.; Bi, X.; Lim, C.J.; Melin, S. Energy input and quality of pellets made from steam-exploded Douglas fir (*Pseudotsuga menziesii*). *Energy Fuels* **2011**, *25*, 1521–1528. [CrossRef]
126. Tooyserkani, Z.; Sokhansanj, S.; Bi, X.; Lim, C.J.; Saddler, J.; Lau, A.; Melin, S.; Lam, P.S.; Kumar, L. Effect of Steam Treatment on Pellet Strength and the Energy Input in Pelleting of Softwood Particles. *ASABE* **2012**, *55*, 2265–2272. [CrossRef]
127. Roy, B.; Kleine-Möllhoff, P.; Dalibard, A. Superheated Steam Torrefaction of Biomass Residues with Valorisation of Platform Chemicals Part—2: Economic Assessment and Commercialisation Opportunities. *Sustainability* **2022**, *14*, 2338. [CrossRef]
128. Zhang, D.; Chen, X.; Qi, Z.; Wang, H.; Yang, R.; Lin, W.; Li, J.; Zhou, W.; Ronsse, F. Superheated steam as carrier gas and the sole heat source to enhance biomass torrefaction. *Bioresour. Technol.* **2021**, *331*, 124955. [CrossRef] [PubMed]
129. Lam, P.S.; Sokhansanj, S.; Bi, X.T.; Lim, C.J.; Larsson, S.H. Drying characteristics and equilibrium moisture content of steam-treated Douglas fir (*Pseudotsuga menziesii* L.). *Bioresour. Technol.* **2012**, *116*, 396–402. [CrossRef] [PubMed]
130. Lam, P.S.; Lam, P.Y.; Sokhansanj, S.; Bi, X.T.; Lim, C.J. Mechanical and compositional characteristics of steam-treated Douglas fir (*Pseudotsuga menziesii* L.) during pelletization. *Biomass Bioenergy* **2013**, *56*, 116–126. [CrossRef]

131. Hanaffi, A.M.; Fuad, M.; Hasan, F.; Ani, F.N. Microwave torrefaction for viable fuel production: A review on theory, affecting factors, potential and challenges. *Fuel* **2019**, *253*, 512–526. [CrossRef]
132. Kang, K.; Nanda, S.; Lam, S.S.; Zhang, T.; Huo, L.; Zhao, L. Enhanced fuel characteristics and physical chemistry of microwave hydrochar for sustainable fuel pellet production via co-densification. *Environ. Res.* **2020**, *186*, 109480. [CrossRef]
133. Satpathy, S.K.; Tabil, L.G.; Meda, V.; Naik, S.N.; Prasad, R. Torrefaction of wheat and barley straw after microwave heating. *Fuel* **2014**, *124*, 269–278. [CrossRef]
134. Amer, M.; Nour, M.; Ahmed, M.; Ookawara, S.; Nada, S.; Elwardany, A. The effect of microwave drying pretreatment on dry torrefaction of agricultural biomasses. *Bioresour. Technol.* **2019**, *286*, 121400. [CrossRef]
135. Yek, P.N.Y.; Osman, M.S.; Wong, C.C.; Wong, C.S.; Kong, S.H.; Sung Sie, T.; Foong, S.Y.; Lam, S.S.; Keey Liew, R. Microwave wet torrefaction: A catalytic process to convert waste palm shell into porous biochar. *Mater. Sci. Energy Technol.* **2020**, *3*, 742–747. [CrossRef]
136. Natarajan, P.; Suriapparao, D.V.; Vinu, R. Microwave torrefaction of Prosopis juliflora: Experimental and modeling study. *Fuel Process. Technol.* **2018**, *172*, 86–96. [CrossRef]
137. Ren, S.; Lei, H.; Wang, L.; Bu, Q.; Wei, Y.; Liang, J.; Liu, Y.; Julson, J.; Chen, S.; Wu, J.; et al. Microwave Torrefaction of Douglas Fir Sawdust Pellets. *Energy Fuels* **2012**, *26*, 5936–5943. [CrossRef]
138. Chen, W.H.; Lin, B.J.; Lin, Y.Y.; Chu, Y.-S.; Ubando, A.T.; Show, P.L.; Ong, H.C.; Chang, J.S.; Ho, S.-H.; Culaba, A.B.; et al. Progress in biomass torrefaction: Principles, applications and challenges. *Prog. Energy Combust. Sci.* **2021**, *82*, 100887. [CrossRef]
139. Tumuluru, J.S.; Ghiasi, B.; Soelberg, N.R.; Sokhansanj, S. Biomass Torrefaction Process, Product Properties, Reactor Types, and Moving Bed Reactor Design Concepts. *Front. Energy Res.* **2021**, *9*, 728140. [CrossRef]
140. Okekunle, P.O. Modelling and simulation of intra-particle heat transfer during biomass torrefaction in a fixed-bed reactor. *Biofuels* **2022**, *13*, 95–104. [CrossRef]
141. Starfelt, F.; Tomas Aparicio, E.; Li, H.; Dotzauer, E. Integration of torrefaction in CHP plants—A case study. *Energy Convers. Manag.* **2015**, *90*, 427–435. [CrossRef]
142. Kumar, L.; Koukoulas, A.A.; Mani, S.; Satyavolu, J. Integrating torrefaction in the wood pellet industry: A critical review. *Energy Fuels* **2017**, *31*, 37–54. [CrossRef]
143. Bach, Q.V.; Nguyen, D.D.; Lee, C.-J. Effect of Torrefaction on Steam Gasification of Biomass in Dual Fluidized Bed Reactor—A Process Simulation Study. *Bioenergy Res.* **2019**, *12*, 1042–1051. [CrossRef]
144. Bandara, J.; Narayana, M. Development of controller for disturbances rejection of torrefaction reactor with high thermal inertia. In Proceedings of the 7th International Multidisciplinary Moratuwa Engineering Research Conference, Virtual, 27–29 July 2021; pp. 292–296. [CrossRef]
145. Direktor, L.B.; Zaichenko, V.M.; Sinelshchikov, V.A. Numerical simulation of power-engineering complex with torrefaction reactor. *High Temp.* **2017**, *55*, 124–130. [CrossRef]
146. Patuzzi, F.; Gasparella, A.; Baratieri, M. Thermochemical and fluid dynamic model of a bench-scale torrefaction reactor. *Waste Biomass Valor.* **2014**, *5*, 165–173. [CrossRef]
147. Ratte, J.; Fardet, E.; Mateos, D.; Héry, J.-S. Mathematical modelling of a continuous biomass torrefaction reactor: TORSPYD™ column. *Biomass Bioenergy* **2011**, *35*, 3481–3495. [CrossRef]
148. Saadon, S.Z.A.H.; Osman, N.B.; Damodaran, M.; Liew, S.E. Torrefaction of Napier Grass and Oil Palm Petiole Waste Using Drop-Type Fixed-Bed Pyrolysis Reactor. *Materials* **2022**, *15*, 2890. [CrossRef] [PubMed]
149. Sarker, T.R.; Nanda, S.; Dalai, A.K.; Meda, V. A Review of Torrefaction Technology for Upgrading Lignocellulosic Biomass to Solid Biofuels. *Bioenergy Res.* **2021**, *14*, 645–669. [CrossRef]
150. Tanoue, K.-I.; Hikasa, K.; Hamaoka, Y.; Yoshinaga, A.; Nishimura, T.; Uemura, Y.; Hideno, A. Heat and mass transfer during lignocellulosic biomass torrefaction: Contributions from the major components-cellulose, hemicellulose, and lignin. *Processes* **2020**, *8*, 959. [CrossRef]
151. Wang, G.; Luo, Y.H.; Deng, J.; Kuang, J.H.; Zhang, Y.L. Pretreatment of biomass by torrefaction. *Chinese Sci Bull* **2011**, *56*, 1442–1448. [CrossRef]
152. Phanphanich, M.; Mani, S. Impact of Torrefaction on the Grindability and Fuel Characteristics of Forest Biomass. *Bioresour. Technol.* **2011**, *102*, 1246–1253. [CrossRef] [PubMed]
153. Huang, C.; Jiang, X.; Shen, X.; Hu, J.; Tang, W.; Wu, X.; Ragauskas, A.; Jameel, H.; Meng, X.; Yong, Q. Lignin-enzyme interaction: A roadblock for efficient enzymatic hydrolysis of lignocellulosics. *Renew. Sustain. Energy Rev.* **2022**, *154*, 111822. [CrossRef]
154. Ribeiro, J.M.C.; Godina, R.; Matias, J.C.d.O.; Nunes, L.J.R. Future Perspectives of Biomass Torrefaction: Review of the Current State-Of-The-Art and Research Development. *Sustainability* **2018**, *10*, 2323. [CrossRef]
155. Torres, R.; Valdez, B.; Beleño, M.T.; Coronado, M.A.; Stoytcheva, M.; García, C.; Rojano, B.A.; Montero, G. Char production with high-energy value and standardized properties from two types of biomass. *Biomass Convers. Biorefin.* **2021**. [CrossRef]
156. Ivanovski, M.; Goricanec, D.; Krope, J.; Urbancl, D. Torrefaction pretreatment of lignocellulosic biomass for sustainable solid biofuel production. *Energy* **2022**, *240*, 122483. [CrossRef]
157. Oyebode, W.A.; Ogunsuyi, H.O. Impact of torrefaction process temperature on the energy content and chemical composition of stool tree (*Alstonia congenisis* Engl) woody biomass. *Curr. Res. Green Sustain. Chem.* **2021**, *4*, 100115. [CrossRef]
158. Zheng, A.; Zhao, Z.; Chang, S.; Huang, Z.; Zhao, K.; Wei, G.; He, F.; Li, H. Comparison of the effect of wet and dry torrefaction on chemical structure and pyrolysis behavior of corncob. *Bioresour. Technol.* **2015**, *176*, 15–22. [CrossRef] [PubMed]

159. Zhang, S.; Chen, T.; Xiong, Y.; Dong, Q. Effects of wet torrefaction on the physicochemical properties and pyrolysis product properties of rice husk. *Energy Convers. Manag.* **2017**, *141*, 403–409. [CrossRef]
160. Poudel, J.; Ohm, T.-I.; Lee, S.-H.; Oh, S.C. A study on torrefaction of sewage sludge to enhance solid fuel qualities. *Waste Management* **2015**, *40*, 112–118. [CrossRef] [PubMed]
161. Chen, C.; Yang, R.; Wang, X.; Qu, B.; Zhang, M.; Ji, G.; Li, A. Effect of in-situ torrefaction and densification on the properties of pellets from rice husk and rice straw. *Chemosphere* **2022**, *289*, 133009. [CrossRef]
162. Mukherjee, A.; Okolie, J.A.; Niu, C.; Dalai, A.K. Experimental and Modeling Studies of Torrefaction of Spent Coffee Grounds and Coffee Husk: Effects on Surface Chemistry and Carbon Dioxide Capture Performance. *ACS Omega* **2022**, *7*, 638–653. [CrossRef]
163. Sidiras, D.K.; Nazos, A.G.; Giakoumakis, G.E.; Politi, D.V. Simulating the Effect of Torrefaction on the Heating Value of Barley Straw. *Energies* **2020**, *13*, 736. [CrossRef]
164. Liu, Y.; Rokni, E.; Yang, R.; Ren, X.; Sun, R.; Levendis, Y.A. Torrefaction of corn straw in oxygen and carbon dioxide containing gases: Mass/energy yields and evolution of gaseous species. *Fuel* **2021**, *285*, 119044. [CrossRef]
165. Sukiran, M.A.; Wan Daud, W.M.A.; Abnisa, F.; Nasrin, A.B.; Astimar, A.A.; Loh, S.K. Individual torrefaction parameter enhances characteristics of torrefied empty fruit bunches. *Biomass Convers. Biorefinery* **2021**, *11*, 461–472. [CrossRef]
166. Kongto, P.; Palamanit, A.; Chaiprapat, S.; Tippayawong, N. Enhancing the fuel properties of rubberwood biomass by moving bed torrefaction process for further applications. *Renew. Energy* **2021**, *170*, 703–713. [CrossRef]
167. Sibiya, N.T.; Oboirien, B.; Lanzini, A.; Gandiglio, M.; Ferrero, D.; Papurello, D.; Bada, S.O. Effect of different pre-treatment methods on gasification properties of grass biomass. *Renew. Energy* **2021**, *170*, 875–883. [CrossRef]
168. Park, J.-H.; Choi, Y.-C.; Lee, Y.-J.; Kim, H.-T. Characteristics of Miscanthus Fuel by Wet Torrefaction on Fuel Upgrading and Gas Emission Behavior. *Energies* **2020**, *13*, 2669. [CrossRef]
169. Gan, M.J.; Lim, W.S.; Ng, H.X.; Ong, M.H.; Gan, S.; Lee, L.Y.; Thangalazhy-Gopakumar, S. Enhancement of Palm Kernel Shell Fuel Properties via Wet Torrefaction: Response Surface, Optimization, and Combustion Studies. *Energy Fuels* **2019**, *33*, 11009–11020. [CrossRef]
170. Chowdhury, Z.Z.; Pal, K.; Johan, R.B.; Dabdawb, W.A.Y.; Ali, M.E.; Rafique, R.F. Comparative evaluation of physiochemical properties of a solid fuel derived from adansonia digitata trunk using torrefaction. *BioResources* **2017**, *12*, 3816–3833. [CrossRef]
171. Wang, X.; Wu, J.; Chen, Y.; Pattiya, A.; Yang, H.; Chen, H. Comparative study of wet and dry torrefaction of corn stalk and the effect on biomass pyrolysis polygeneration. *Bioresour. Technol.* **2018**, *258*, 88–97. [CrossRef]
172. Bach, Q.V.; Tran, K.Q. Dry and wet torrefaction of woody biomass—A comparative study on combustion kinetics. *Energy Proc.* **2015**, *75*, 150–155. [CrossRef]
173. González-Arias, J.; Gómez, X.; González-Castaño, M.; Sánchez, M.E.; Rosas, J.G.; Cara-Jiménez, J. Insights into the product quality and energy requirements for solid biofuel production: A comparison of hydrothermal carbonization, pyrolysis and torrefaction of olive tree pruning. *Energy* **2022**, *238*, 122022. [CrossRef]
174. Kanwal, S.; Munir, S.; Chaudhry, N.; Sana, H. Physicochemical characterization of Thar coal and torrefied corn cob. *Energy Explor. Exploit.* **2019**, *37*, 1286–1305. [CrossRef]
175. Bai, X.; Wang, G.; Sun, Y.; Yu, Y.; Liu, J.; Wang, D.; Wang, Z. Effects of combined pretreatment with rod-milled and torrefaction on physicochemical and fuel characteristics of wheat straw. *Bioresour. Technol.* **2018**, *267*, 38–45. [CrossRef]
176. Chen, D.; Gao, A.; Cen, K.; Zhang, J.; Cao, X.; Ma, Z. Investigation of biomass torrefaction based on three major components: Hemicellulose, cellulose, and lignin. *Energy Convers. Manag.* **2018**, *169*, 228–237. [CrossRef]
177. Tumuluru, J.S.; Sokhansanj, S.; Hess, J.R.; Wright, C.T.; Boardman, R.D. A review on biomass torrefaction process and product properties for energy applications. *Ind. Biotechnol.* **2011**, *7*, 384–401. [CrossRef]
178. Jian, J.; Lu, Z.; Yao, S.; Li, X.; Song, W. Comparative Study on Pyrolysis of Wet and Dry Torrefied Beech Wood and Wheat Straw. *Energy Fuels* **2019**, *33*, 3267–3274. [CrossRef]
179. Viegas, C.; Nobre, C.; Correia, R.; Gouveia, L.; Gonçalves, M. Optimization of biochar production by co-torrefaction of microalgae and lignocellulosic biomass using response surface methodology. *Energies* **2021**, *14*, 7330. [CrossRef]
180. Sidiras, D.; Batzias, F.; Ranjan, R.; Tsapatsis, M. Simulation and optimization of batch autohydrolysis of wheat straw to monosaccharides and oligosaccharides. *Bioresour. Technol.* **2011**, *102*, 10486–10492. [CrossRef] [PubMed]
181. Cheng, X.; Huang, Z.; Wang, Z.; Ma, C.; Chen, S. A novel onsite wheat straw pretreatment method: Enclosed torrefaction. *Bioresour. Technol.* **2019**, *281*, 48–55. [CrossRef]
182. Syu, F.-S.; Chiueh, P.-T. Process simulation of rice straw torrefaction. Sustain. *Environ. Res.* **2012**, *22*, 177–183.
183. Chang, S.H. Rice Husk and Its Pretreatments for Bio-oil Production via Fast Pyrolysis: A Review. *Bioenergy Res.* **2020**, *13*, 23–42. [CrossRef]
184. Mandefro, D.; Jabasingh, S.A. A study on the torrefaction of rice husk as an attempt to enhance its energy content. *J. Sci. Ind. Res.* **2021**, *80*, 87–90.
185. Tsai, W.-T.; Jiang, T.-J.; Tang, M.-S.; Chang, C.-H.; Kuo, T.-H. Enhancement of thermochemical properties on rice husk under a wide range of torrefaction conditions. *Biomass Convers. Biorefin.* **2021**, 1–10. [CrossRef]
186. Wang, M.; Wei, J.; Zhang, T.; Ding, K.; Xu, D.; Li, B.; Wang, J.; Zhang, H.; Zhang, S. Effects of dry/wet torrefaction pretreatments on the combustion reaction characteristics of rice husk, Nongye Gongcheng Xuebao. *Trans. Chin. Soc. Agric. Eng.* **2022**, *38*, 236–243. [CrossRef]

187. Lam, P.S.; Sokhansanj, S.; Bi, X.T.; Lim, C.J. Colorimetry applied to steam-treated biomass and pellets made from western douglas fir (*Pseudotsuga menziesii* L.). *Trans. ASABE* **2012**, *55*, 673–678. [CrossRef]
188. Anukam, A.; Mamphweli, S.; Okoh, O.; Reddy, P. Influence of torrefaction on the conversion efficiency of the gasification process of sugarcane bagasse. *Bioengineering* **2017**, *4*, 22. [CrossRef] [PubMed]
189. Matali, S.; Rahman, N.A.; Idris, S.S.; Yaacob, N.; Alias, A.B. Lignocellulosic biomass solid fuel properties enhancement via torrefaction. *Procedia Eng.* **2018**, *148*, 671–678. [CrossRef]
190. Peng, J.H.; Bi, X.T.; Sokhansanj, S.; Lim, C.J. Torrefaction and densification of different species of softwood residues. *Fuel* **2013**, *111*, 411–421. [CrossRef]
191. Vashishtha, M.; Patidar, K. Property Enhancement of Mustard Stalk Biomass by Torrefaction: Characterization and Optimization of Process Parameters Using Response Surface Methodology. *Mater. Sci. Energy Technol.* **2021**, *4*, 432–441. [CrossRef]
192. Park, S.; Jeong, H.-R.; Shin, Y.-A.; Kim, S.-J.; Ju, Y.-M.; Oh, K.-C.; Cho, L.-H.; Kim, D. Performance optimisation of fuel pellets comprising pepper stem and coffee grounds through mixing ratios and torrefaction. *Energies* **2021**, *14*, 4667. [CrossRef]
193. Ozonoh, M.; Oboirien, B.O.; Daramola, M.O. Optimization of process variables during torrefaction of coal/biomass/waste tyre blends: Application of artificial neural network & response surface methodology. *Biomass Bioenerg.* **2020**, *143*, 105808.
194. Mukhtar, H.; Feroze, N.; Muhammad, H.; Munir, S.; Javed, F.; Kazmi, M. Torrefaction process optimization of agriwaste for energy densification. *Energy Sources Part A Recover. Util. Environ. Eff.* **2020**, *42*, 2526–2544. [CrossRef]
195. Aguado, R.; Cuevas, M.; Pérez-Villarejo, L.; Martínez-Cartas, M.L.; Sánchez, S. Upgrading almond-tree pruning as a biofuel via wet torrefaction. *Renew. Energy* **2020**, *145*, 2091–2100. [CrossRef]
196. Swiechowski, K.; Stegenta-Dabrowska, S.; Liszewski, M.; Babelewski, P.; Koziel, J.A.; Białowiec, A. Oxytree pruned biomass torrefaction: Process kinetics. *Materials* **2019**, *12*, 3334. [CrossRef]
197. Chen, W.-H.; Aniza, R.; Arpia, A.A.; Lo, H.-J.; Hoang, A.T.; Goodarzi, V.; Gao, J. A comparative analysis of biomass torrefaction severity index prediction from machine learning. *Appl. Energy* **2022**, *324*, 119689. [CrossRef]
198. García Nieto, P.J.; García-Gonzalo, E.; Sánchez Lasheras, F.; Paredes-Sánchez, J.P.; Riesgo Fernández, P. Forecast of the higher heating value in biomass torrefaction by means of machine learning techniques. *J. Comput. Appl. Math.* **2019**, *357*, 284–301. [CrossRef]
199. García Nieto, P.J.; García-Gonzalo, E.; Paredes-Sánchez, J.P.; Bernardo Sánchez, A.; Menéndez Fernández, M. Predictive modelling of the higher heating value in biomass torrefaction for the energy treatment process using machine-learning techniques. *Neural Comput. Appl.* **2019**, *31*, 8823–8836. [CrossRef]
200. Di Blasi, C.; Lanzetta, M. Intrinsic kinetics of isothermal xylan degradation in inert atmosphere. *J. Anal. Appl. Pyrolysis* **1997**, *40–41*, 287–303. [CrossRef]
201. Prins, M.J.; Ptasinski, K.J.; Janssen, F.J. Torrefaction of wood: Part 1. Weight loss kinetics. *J. Anal. Appl. Pyrolysis* **2006**, *77*, 28–34. [CrossRef]
202. Onsree, T.; Tippayawong, N. Analysis of reaction kinetics for torrefaction of pelletized agricultural biomass with dry flue gas. *Energy Rep.* **2020**, *6*, 61–65. [CrossRef]
203. Ikegwu, U.M.; Ozonoh, M.; Daramola, M.O. Kinetic Study of the Isothermal Degradation of Pine Sawdust during Torrefaction Process. *ACS Omega* **2021**, *6*, 10759–10769. [CrossRef]
204. Soria-Verdugo, A.; Cano-Pleite, E.; Panahi, A.; Ghoniem, A.F. Kinetics mechanism of inert and oxidative torrefaction of biomass. *Energy Convers. Manag.* **2022**, *267*, 115892. [CrossRef]
205. Joshi, Y.; De Vries, H.; Woudstra, T.; De Jong, W. Torrefaction: Unit operation modelling and process simulation. *Appl. Therm. Eng.* **2015**, *74*, 83–88. [CrossRef]
206. Soponpongpipat, N.; Sae-Ueng, U. The effect of biomass bulk arrangements on the decomposition pathways in the torrefaction process. *Renew. Energy* **2015**, *81*, 679–684. [CrossRef]
207. Sasongko, D.; Nugraha, N.B.; Rasrendra, C.B.; Indarto, A. Simulation of temperature and reaction time prediction of the torrefaction process: Case of hard-wood biomass. *Int. J. Ambient Energy* **2018**, *39*, 108–116. [CrossRef]
208. Chai, M.; Xie, L.; Yu, X.; Zhang, X.; Yang, Y.; Rahman, M.M.; Blanco, P.H.; Liu, R.; Bridgwater, A.V.; Cai, J. Poplar wood torrefaction: Kinetics, thermochemistry and implications. *Renew. Sustain. Energy Rev.* **2021**, *143*, 110962. [CrossRef]
209. Chen, W.-H.; Cheng, C.-L.; Show, P.-L.; Ong, H.C. Torrefaction performance prediction approached by torrefaction severity factor. *Fuel* **2019**, *251*, 126–135. [CrossRef]
210. Silveira, E.A.; Macedo, L.; Commandré, J.-M.; Candelier, K.; Rousset, P. Potassium impregnation assessment of mild biomass pyrolysis by catalytic torrefaction severity factor. In Proceedings of the 29th European Biomass Conference and Exhibition, Online, 26–29 April 2021; pp. 1015–1019.
211. Zhang, C.; Ho, S.H.; Chen, W.H.; Xie, Y.; Liu, Z.; Chang, J.S. Torrefaction performance and energy usage of biomass wastes and their correlations with torrefaction severity index. *Appl. Energy* **2018**, *220*, 598–604. [CrossRef]
212. Manouchehrinejad, M.; Mani, S. Process simulation of an integrated biomass torrefaction and pelletization (iBTP) plant to produce solid biofuels. *Energy Convers. Manag. X* **2019**, *1*, 100008. [CrossRef]
213. Awang, A.H.; Abdulrazik, A.; Noor, A.M.; Nafsun, A.I. Modelling and optimization of torrefied pellet fuel production. *Pertanika J. Sci. Technol.* **2019**, *27*, 2139–2152.
214. Jamin, N.A.; Samad, N.A.F.A.; Saleh, S. Anhydrous weight loss kinetics model development for torrefied green waste. *IOP Conf. Ser. Mater. Sci. Eng.* **2019**, *702*, 012008. [CrossRef]

215. Brachi, P.; Chirone, R.; Miccio, F.; Miccio, M.; Ruoppolo, G. Entrained-flow gasification of torrefied tomato peels: Combining torrefaction experiments with chemical equilibrium modeling for gasification. *Fuel* **2018**, *220*, 744–753. [CrossRef]
216. Mobini, M.; Meyer, J.-C.; Trippe, F.; Sowlati, T.; Fröhling, M.; Schultmann, F. Assessing the integration of torrefaction into wood pellet production. *J. Clean. Prod.* **2014**, *78*, 216–225. [CrossRef]
217. Lee, S.M.; Lee, J.-W. Optimization of biomass torrefaction conditions by the Gain and Loss method and regression model analysis. *Bioresour. Technol.* **2014**, *172*, 438–443. [CrossRef]
218. Duan, H.; Zhang, Z.; Rahman, M.M.; Guo, X.; Zhang, X.; Cai, J. Insight into torrefaction of woody biomass: Kinetic modeling using pattern search method. *Energy* **2020**, *201*, 117648. [CrossRef]
219. Brighenti, M.; Grigiante, M.; Antolini, D.; Di Maggio, R. An innovative kinetic model dedicated to mild degradation (torrefaction) of biomasses. *Appl. Energy* **2017**, *206*, 475–486. [CrossRef]
220. Oh, K.C.; Kim, J.; Park, S.Y.; Kim, S.J.; Cho, L.H.; Lee, C.G.; Roh, J.; Kim, D.H. Development and validation of torrefaction optimization model applied element content prediction of biomass. *Energy* **2021**, *214*, 119027. [CrossRef]
221. Nhuchhen, D.; Afzal, M. HHV predicting correlations for torrefied biomass using proximate and ultimate analyses. *Bioengineering* **2017**, *4*, 7. [CrossRef] [PubMed]
222. Xu, J.; Huang, M.; Hu, Z.; Zhang, W.; Li, Y.; Yang, Y.; Zhou, Y.; Zhou, S.; Ma, Z. Prediction and modeling of the basic properties of biomass after torrefaction pretreatment. *J. Anal. Appl. Pyrolysis* **2021**, *159*, 105287. [CrossRef]
223. Chen, W.-H.; Lo, H.-J.; Aniza, R.; Lin, B.-J.; Park, Y.-K.; Kwon, E.E.; Sheen, H.-K.; Alan, L.; Grafilo, D.R. Forecast of glucose production from biomass wet torrefaction using statistical approach along with multivariate adaptive regression splines, neural network and decision tree. *Appl. Energy* **2022**, *324*, 119775. [CrossRef]
224. Mäkelä, M.; Yoshikawa, K. Simulating hydrothermal treatment of sludge within a pulp and paper mill. *Appl. Energy* **2016**, *173*, 177–183. [CrossRef]
225. Yek, P.N.Y.; Cheng, Y.W.; Liew, R.K.; Wan Mahari, W.A.; Ong, H.C.; Chen, W.-H.; Peng, W.; Park, Y.-K.; Sonne, C.; Kong, S.H.; et al. Progress in the torrefaction technology for upgrading oil palm wastes to energy-dense biochar: A review. *Renew. Sustain. Energy Rev.* **2021**, *151*, 111645. [CrossRef]
226. Sun, Y.; Tong, S.; Li, X.; Wang, F.; Hu, Z.; Dacres, O.D.; Edreis, E.M.A.; Worasuwannarak, N.; Sun, M.; Liu, H.; et al. Gas-pressurized torrefaction of biomass wastes: The optimization of pressurization condition and the pyrolysis of torrefied biomass. *Bioresour. Technol.* **2021**, *319*, 124216. [CrossRef]